ARMY RESEARCH LABORATORY

Failure Analysis and Mechanical Tests of Failed Aluminum Alloy 7277 Rivets on Armored Vehicle Launched Bridges

Howard E. Horner

ARL-TR-1195 September 1996

NOTICES

Destroy this report when it is no longer needed. DO NOT return it to the originator.

Additional copies of this report may be obtained from the National Technical Information Service, U.S. Department of Commerce, 5285 Port Royal Road, Springfield, VA 22161.

The findings of this report are not to be construed as an official Department of the Army position, unless so designated by other authorized documents.

The use of trade names or manufacturers' names in this report does not constitute indorsement of any commercial product.

REPORT DOCUMENTATION PAGE

Form Approved
OMB No. 0704-0188

1. AGENCY USE ONLY *(Leave blank)*	2. REPORT DATE	3. REPORT TYPE AND DATES COVERED
	September 1996	Final, April 1994 - September 1995

4. TITLE AND SUBTITLE
Failure Analysis and Mechanical Tests of Failed Aluminum Alloy 7277 Rivets on Armored Vehicle Launched Bridges

5. FUNDING NUMBERS
PR: 1L162618AH80

6. AUTHOR(S)
Howard E. Horner

7. PERFORMING ORGANIZATION NAME(S) AND ADDRESS(ES)
U.S. Army Research Laboratory
ATTN: AMSRL-WM-MA
Fort Belvoir, VA 22060-5812

8. PERFORMING ORGANIZATION REPORT NUMBER
ARL-TR-1195

9. SPONSORING/MONITORING AGENCY NAMES(S) AND ADDRESS(ES)

10.SPONSORING/MONITORING AGENCY REPORT NUMBER

11. SUPPLEMENTARY NOTES

12a. DISTRIBUTION/AVAILABILITY STATEMENT
Approved for public release; distribution is unlimited.

12b. DISTRIBUTION CODE

13. ABSTRACT *(Maximum 200 words)*

A number of the manufactured buttonheads of the 0.75-in-diameter hot-driven aluminum rivets (made of alloy 7277) were found to have fallen off Class 60 Armored Vehicle Launched Bridges (AVLB) that had been employed in Saudi Arabia during Operation Desert Storm. The presence of white corrosion deposits observed on the fractured surfaces of the failed heads indicated corrosion. The objectives of the work were to determine the cause of rivet head failures and conduct a number of mechanical tests to evaluate the integrity of the corroded rivets without their heads or with cracked heads.

Corroded aluminum rivet samples were obtained, examined, and tested. The rivet head failures were caused by stress corrosion cracking initiated in the sharp head-to-shank fillets that acted as stress raisers. Depending on the amounts of the white corrosion products formed, they bound the headless rivet shanks in the rivet holes. No failures similar to those in the rivet heads were found in the rivet shanks. With corroded shanks remaining in the rivet holes of the bridge parts and with major stresses acting in shear on the shanks, the corroded rivet shanks or the crack rivet buttonheads can still allow the bridge to function satisfactorily until the corroded aluminum rivets are replaced.

14. SUBJECT TERMS
aluminum alloy 7277, failure analysis, stress corrosion cracking, rivets, bridges, mechanical tests

15. NUMBER OF PAGES
76

16. PRICE CODE

17. SECURITY CLASSIFICATION OF REPORT	18. SECURITY CLASSIFICATION OF THIS PAGE	19. SECURITY CLASSIFICATION OF ABSTRACT	20. LIMITATION OF ABSTRACT
UNCLASSIFIED	UNCLASSIFIED	UNCLASSIFIED	UL

INTENTIONALLY LEFT BLANK.

ACKNOWLEDGMENT

The assistance provided by Mr. Dario A. Emeric of the Coatings Team, Engineering Materials and Coatings Branch (AMSRL-MA-E), U.S. Army Research Laboratory (ARL), on the corrosion aspects is acknowledged.

INTENTIONALLY LEFT BLANK.

TABLE OF CONTENTS

		Page
	ACKNOWLEDGMENT	iii
	LIST OF FIGURES	vii
	LIST OF TABLES	xi
1.	INTRODUCTION	1
1.1	Samples	4
1.2	Test Methods	4
2.	RESULTS	4
2.1	Preliminary Examination of a Failed Rivet Head Sample to Determine the Primary Cause of Aluminum Head Failures	4
2.2	Metallurgical Evaluation of an Aluminum Rivet Sample With Less Corrosion	6
2.3	Metallurgical Examination of Several Corroded AVLB Aluminum Component Samples	10
2.4	Shear Tests of Six AVLB Aluminum Rivet Samples	12
2.5	Mechanical Properties of Several Aluminum Alloy 7277 Rivet Samples	20
2.6	Clamping and Breaking Loads of Six Installed Aluminum Rivets From AVLB	22
2.7	Pull Tests on Two New AVLB Installed Aluminum Rivet Specimens	27
2.8	Tests on Two "Good" and Two "Bad" AVLB Rivet Specimens	27
2.9	Clamping and Breaking Loads of New Hot-Driven AVLB Aluminum Rivets	33
2.10	Pull Tests on 11 AVLB Aluminum Rivet Samples From ANAD	36
2.11	Push Tests on Corroded AVLB Aluminum Rivets Without the Manufactured Heads	39
2.12	Initial Visual Inspection of a Corroded AVLB (MLC-60 Tons)	45
2.13	Push-Out Tests of Aluminum Rivets From Corroded AVLB	48
2.14	Metallurgical Examination of the Fractures of Several Failed Major Aluminum Components of Corroded AVL Bridge After the Overload Test	51
3.	CONCLUSIONS	60
4.	RECOMMENDATIONS	63
	DISTRIBUTION LIST	67

INTENTIONALLY LEFT BLANK.

LIST OF FIGURES

Figure		Page
1.	AVLB (at right) in the scissoring formation from the bridge launcher (at left)	2
2.	A view of the splice joint in the bottom chord of the AVLB from SWA, showing a failed aluminum rivet with its head already popped off	2
3.	A view of a top chord connector of the AVLB from SWA, showing two failed aluminum rivets with their heads fallen off	3
4.	Side view of a failed aluminum rivet head sample received for failure analysis	5
5.	A view of the fracture surface of the same rivet head in Figure 4	5
6.	As-polished microstructure of the failed aluminum rivet head showing a small secondary crack in the fracture	7
7.	Etched microstructure of the same area in Figure 6 revealing that the crack is predominately intergranular, indicative of stress corrosion cracking	7
8.	A view of a large aluminum rivet removed from a forged aluminum center hinge of one AVLB from SWA stored at ANAD	9
9.	As-polished microstructure of the aluminum rivet in Figure 8	9
10.	Etched microstructure of the same area in Figure 9	10
11.	Large corroded hole (A) on top surface of the top chord angle section cut from AVLB center panel dismantled at ANAD	11
12.	Matched half sections of the corroded sample in Figure 11	11
13.	As-polished microstructure at the bottom of the corroded hole in Figure 11	12
14.	A section of the aluminum rivet shank still in the rivet hole of the spacer bar removed from the AVLB center panel assembly dismantled at ANAD	13
15.	Etched cross sections of the sample in Figure 14 to show the end of the rivet shank still in the rivet hole of the spacer bar	13
16.	As-polished microstructure of the rivet shank (right) and spacer bar at the interface in the rivet hole of the bar in Figure 15	14
17.	A 4-in-long large aluminum rivet sample with heavy deposits of white corrosion products on the surface of its shank	14
18.	As-polished microstructure of a small corroded area on the surface of the rivet shank in Figure 17 covered with thick corrosion products	15

Figure		Page
19.	Etched microstructure of the same area in Figure 8	15
20.	A shear aluminum test specimen cut from AVLB panel assembly, showing the rivet at the low position	17
21.	A shear aluminum test specimen showing the rivet at the high position	17
22.	A typical setup of the AVLB rivet shear test specimen on the testing machine for double shearing of the rivet shank	18
23.	View of "Bad" (left) and "Good" rivets after the shear tests	19
24.	Cross sections of AVLB corroded rivet heads sectioned in two after the shear tests	19
25.	View of the rivet holes in the angle vertical leg on left and in the girder plate plunger on right after the shear test	20
26.	Typical pull test specimen with three 0.5-in-diameter holes drilled 120° apart around the rivet head on one side of the specimen	23
27.	Side view of the pull test specimen with the 0.5-in-diameter steel dowel pins already inserted in the drilled holes of the angle legs and girder plate	23
28.	Sketch of pull tests to pull the rivet in tension by applying compression load on the dowel pins (top and bottom views)	24
29.	Enlarged view of the fracture surface of the rivet head (specimen C) that broke at the head-to-shank fillet after the pull test, revealing the darkened area of the crack because of corrosion (stress corrosion cracking)	26
30.	A view of the rivet (specimen D) with the sheared driven end (left) after the pull test	26
31.	A view of the cross section of the installed rivet showing a large crack in the fillet	28
32.	A view of the rivet that was rough cut in half lengthwise in the top connector of the AVLB, thus revealing large cracks in the head	28
33.	Same rivet in Figure 32, except with as-polished surface of the cut areas	29
34.	A view of two rivet heads (specimen B on left and specimen D on right) after the shear tests	30
35.	Enlarged view of specimen A "Good" rivet that sheared at its driven end through the rivet hole of the angle leg during the pull test	32
36.	Enlarged view of the fracture surface under the head of specimen C "Bad" rivet after the pull test	32
37.	Enlarged view of two quarter sections of specimen D "Bad" rivet in Figure 34	34

Figure		Page
38.	Matched cross sections of the right quarter section in Figure 36	34
39.	An example of the shearing at the flat countersunk head of unpainted 1,025° F rivet sample	37
40.	Enlarged views of the fracture surface under the buttonhead of four rivet samples after the pull tests, revealing the extent of cracks (darkened areas) observed due to corrosion	40
41.	Enlarged views of the surface under the buttonhead of four rivet samples after the pull tests, revealing the extent of the cracks (darkened areas) observed	41
42.	A view of the headless AVLB aluminum rivet samples 10 (left) and 15 after the plunger push tests, revealing the condition of the corroded rivet shanks	44
43.	Enlarged view of the etched cross sections of the corroded AVLB rivet samples 10 (top) and 15, revealing stress corrosion cracks (dark curved lines) in the headless ends (arrows A and B) where the rivet buttonheads were sawed off	45
44.	As-polished microstructure of stress corrosion cracks on the shank of corroded rivet sample 10 near the fillet	46
45.	Etched microstructure of the same area in Figure 44, showing the grain flow formed by the head-forming operation	47
46.	As-polished microstructure of stress corrosion cracks on the shank of the corroded rivet sample 15 near the fillet area	48
47.	Etched microstructure of the same area in Figure 46, showing the grain flow formed by the head-forming operation	49
48.	A view of the special push load jig after the fabrication	50
49.	Overall view of the special load jig clamped to the top outboard male connector of the AVLB female center panel assembly by means of bolts and plates	51
50.	Closeup view of the special jig in Figure 49 showing the placement of the 0.5-in-diameter steel pin (with two strain gauges) between the headless end of the rivet and the plunger end of the hydraulic cylinder	52
51.	A view of the white corrosion products on the surface of the shank of no. 1 headless corroded rivet at left, no. 5 rivet in middle, and no. 7 rivet at right	54
52.	View of broken inboard female center hinge eyes	54
53.	View of broken outboard bottom chord male connector eyes from the female center panel assembly after the failure test	55
54.	View of broken inboard bottom chord male connector eyes from the female center panel assembly	55

Figure		Page
55.	Closeup view of a small fatigue crack (arrow) at A in Figure 52	56
56.	Closeup view of a small fatigue cracks (top edge) at B in Figure 52 after the eye piece broke from the forged female center hinge at 115-ton load	56
57.	Closeup view of a small fatigue crack (arrow) at A in Figure 53 where it was initiated at the sharp machined fillet (straight edge)	57
58.	Closeup view of a small fatigue crack (arrow) at B in Figure 53 where it was initiated at the sharp machined fillet (straight edge)	57
59.	Closeup view of the fracture at A in Figure 54 showing small fatigue cracks (top edge) in the eyehole where the brittle fracture initiated in the connector	58
60.	Prior cracks at first countersunk hole of the inner outboard bottom chord angles of the male center panel assemblies that had occurred during the fatigue test of 3,000 simulated MLC-70 ton crossings	58
61.	Closeup view of the fracture at the rivet hole of S/N 176 cracked angled in Figure 60, showing small fatigue cracks at upper corners of the hole	59
62.	View of the corroded surfaces of the inner outboard bottom chord angle samples cut from the male center panel assemblies S/N 176 and S/N 178 (left) in Figure 60	59
63.	Microstructure of the fracture at A of the broken inboard female center hinge eye in Figure 1	61
64.	Microstructure of the corroded surface (top edge) near the fracture of the cracked bottom chord angle from the male center panel assembly S/N 176 in Figure 62	61
65.	Microstructure of the corroded surface (top edge) near the fracture of the cracked bottom hard angle from the male center panel assembly S/N 178	62
66.	A view of the aluminum Huckbolt fastener	64
67.	A view of the Huckbolt fastener installed in the rivet holes of the aluminum parts prior to swaging of the collar	64
68.	Closeup view of the fully swaged collar of the Huckbolt fastener after the installation	65

LIST OF TABLES

Table		Page
1.	Composition of the Failed Aluminum Rivet Head Sample	6
2.	Shear Property of Six AVLB Corroded Rivet Specimens	18
3.	Mechanical Properties of Aluminum Alloy 7277 Rivet Samples	21
4.	Clamping and Breaking Loads of Six AVLB Rivet Specimens	25
5.	Breaking Loads of New Aluminum Rivets by Pull Tests	29
6.	Description of Aluminum Rivet Samples for AVLB Female Center Panel	29
7.	Test Results on "Good" and "Bad" AVLB Rivet Specimens	31
8.	Clamping Load Determination for New Hot-Driven AVLB Aluminum Alloy Rivets	35
9.	Breaking Load for New Hot-Driven AVLB Aluminum Alloy Rivets (Pull Tests)	36
10.	Description of AVLB Aluminum Rivet Samples From ANAD	38
11.	Pull Tests on AVLB Rivet Samples	39
12.	Push Tests of Corroded AVLB Rivets Without Their Manufactured Heads	43
13.	Description of the Aluminum Rivets Tested and Results of the Push-Out Tests	53

INTENTIONALLY LEFT BLANK.

1. INTRODUCTION

At the Anniston Army Depot (ANAD), AL, a number of large aluminum rivets on several scissoring-type aluminum Class 60 Armored Vehicle Launched Bridges (AVLBs) (see Figure 1), that were brought back to the United States from Southwest Asia (SWA), were found with their manufactured buttonhead already fallen off. The AVLBs were sent back by ships to the United States from Saudi Arabia and Kuwait shortly after the Operation Desert Storm War in early 1991. Before they could reenter in the United States, they were washed down with high pressure spray using seawater to remove soil and insects. The AVLBs were stored out in the field at ANAD for a period of time awaiting repair and refurbishment to the serviceable/operational condition. The problem with the aluminum rivets without heads was discovered when several AVLBs from SWA were to be retrieved from the field for overhaul. Not all AVLBs from SWA at ANAD exhibited this problem. Preliminary visual examination of the failed rivet heads done at ANAD revealed that the surface of the fracture was covered with white corrosion products (see Figures 2 and 3 for examples).

The AVLB is a girder bridge constructed mainly of a high-strength aluminum alloy. The structural system is composed of boxed sections with treads, transverse braces, curbings, supports, and connecting hardware. The bridge consists of two wide treadways connected transversely by braces. Each treadway (two center and two ramp end sections) is hinged in the middle (forged aluminum center hinges) so that the bridge can be folded in the scissor configuration and normally carried atop a heavily armored vehicle bridge launcher such as modified M-48A5 or M-60A1 chassis tanks. The bridge is transportable and maneuverable. It can be deployed to cross ravines, gullies, enemy-placed obstacles, creeks, and rivers. It can be hydraulically launched and/or retrieved from either end by an operator in the bridge launcher. With an overall length of 63 ft, it is capable of carrying Class 60 tracked and wheeled vehicle loads over a 60-ft gap. The heavier and wider M1A1 main battle tank can cross the AVLB over a 50-ft gap for Class 70 load.

Welding is not used in the bridge fabrication because aluminum alloy 2014-T6 used will lose its structural strength when heated. Therefore, the major aluminum bridge components, such as the bottom and top chord angles, forged center hinges and connectors, and girder plates, are riveted together rather than welded. The treads of the bridge are made of extruded aluminum deck panels that are bolted with steel bolts and nuts on top of the boxed sections to form the treadways for the vehicles to ride on the bridge over the gap. The rivets used have mainly 0.75-in diameters of different lengths and are made of

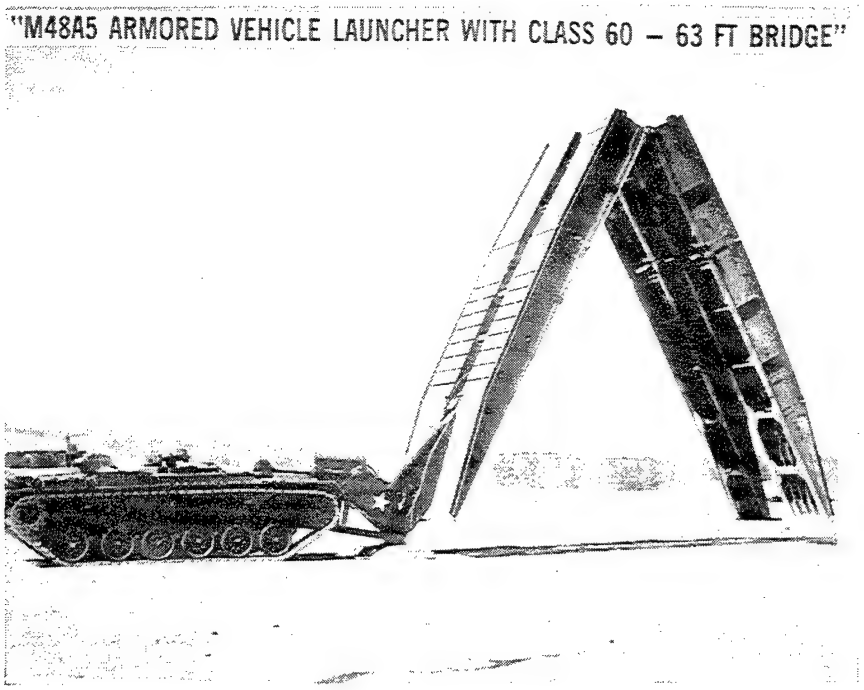

Figure 1. AVLB (at right) in the scissoring formation from the bridge launcher (at left).

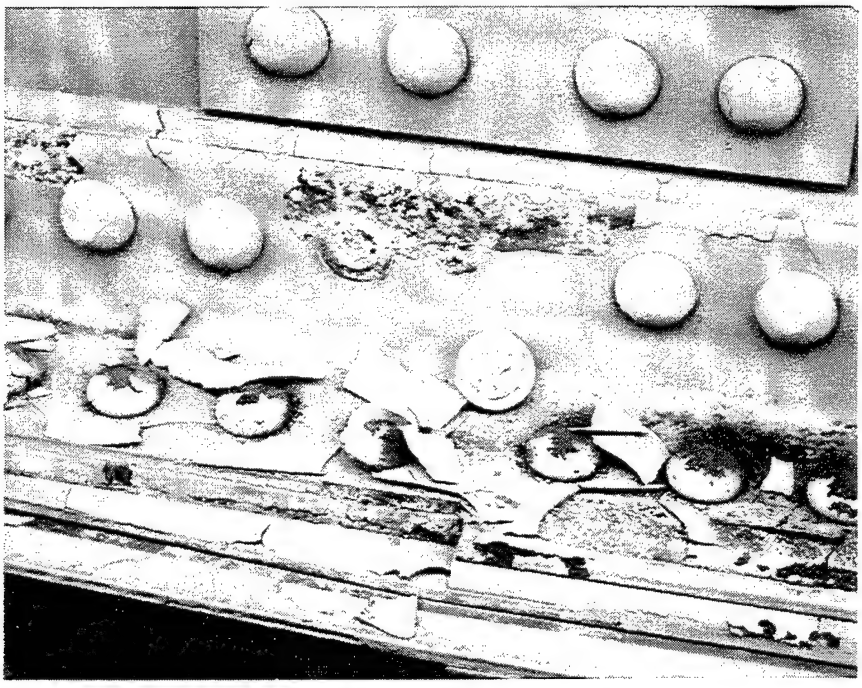

Figure 2. A view of the splice joint in the bottom chord of the AVLB from SWA, showing a failed aluminum rivet with its head already popped off. Note the white areas of the corrosion products formed on the surfaces of the fracture under the failed head as well as on the structural angle where the paint coating had flaked off.

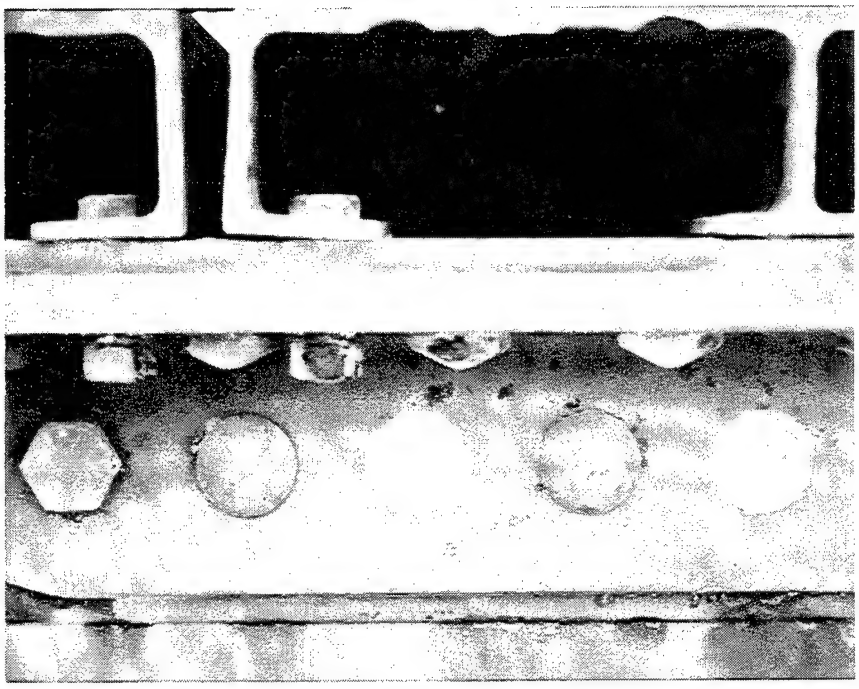

Figure 3. A view of a top chord connector of the AVLB from SWA, showing two failed aluminum rivets with their head already fallen off. The white circular areas are the corrosion products formed under the head at the shoulder and crack fracture. Note the steel bolt at far left which apparently was used to replace the rivet that failed earlier.

aluminum alloy 7277 per MIL-R-12221,[1] which covers solid aluminum alloy 7277 rivets for structural use. Both buttonhead and flat-top countersunk head rivets are used on the bridge. They are hot-driven at elevated temperature (between 850° F and 975° F) so that high shear strength can be developed by natural aging—hence, the reason for using them on the AVLBs.

In this work, the probable cause of the aluminum rivet head failures by corrosion was determined. Because the AVLBs from SWA will be overhauled, the integrity of the corroded rivets with or without the head needs to be evaluated in order to determine the extent of repairs to be made on those bridges at ANAD. In this case, special tests, which are described later in this report, were performed on corroded and noncorroded rivet samples to obtain pertinent data.

[1]U.S. Army Belvoir Research and Development Center. "Rivets, Solid: Aluminum Alloy 7277." MIL-R-12221D(ME), Fort Belvoir, VA, 25 February 1985.

All of the work on the corroded aluminum rivets were done for the Bridge Division of the Mobility Technology Center-Belvoir, U.S. Army Tank-Automotive and Armaments Command (TACOM), Fort Belvoir, VA, which has the technical responsibility for the AVLB.

1.1 Samples. A number of 0.75-in-diameter aluminum rivet samples and a few corroded aluminum component samples were removed from several AVLBs from SWA at ANAD and sent to Belvoir for metallurgical evaluations and tests. New aluminum alloy 7277 rivets used at ANAD for the bridge repairs were also sent as samples to Belvoir for tests. These samples are described in more detail in the Results section for the series of work performed.

1.2 Test Methods. A series of special tests was designed and conducted on the AVLB aluminum rivet samples as needed in order to obtain pertinent data. The data were used to evaluate the integrity of the used corroded and noncorroded rivets in comparison with the new rivets. The special tests used are described in more detail in the Results section for the series of work performed.

2. RESULTS

The results given below cover the series of work performed on the AVLB aluminum samples.

2.1 Preliminary Examination of a Failed Rivet Head Sample to Determine the Primary Cause of Aluminum Rivet Head Failures. A failed manufactured head sample of the aluminum buttonhead rivet was received from ANAD. It had fallen off from one of the AVLBs from SWA at ANAD. Figures 4 and 5 are two views of the failed rivet head sample. The head broke off at the head-to-shank fillet under the head shoulder. The white deposits seen on the surface of the fracture, shoulder surface, and head surface under the loose paint coating were the corrosion products that had formed for a period of time before the head fell off. The products were identified by x-ray diffraction analysis as aluminum hydroxide. Chlorine in a small amount was detected in the products, by x-ray fluorescence analysis, which would indicate the presence of seawater, possibly from high-pressure spraying with seawater for washing down the AVLBs from SWA. In addition, soil and dust in Saudi Arabia and Kuwait were known to contain high-chlorine contents, also contributing in part to the chlorine detected in the corrosion products.

The results of a semi-quantitative chemical analysis by x-ray fluorescence method on the head sample, given in Table 1, indicated that the failed rivet was made of aluminum alloy 7277 as specified. Figures 6

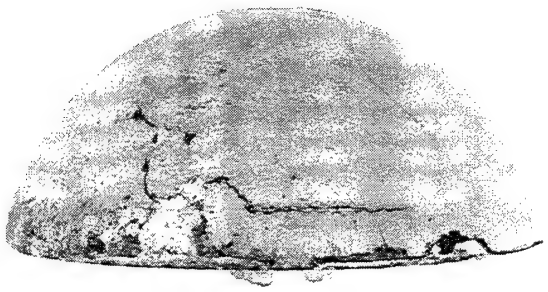

Figure 4. Side view of a failed aluminum rivet head sample received for failure analysis. The rivet shank of the failed rivet was not included for analysis. The white corrosion deposit can be seen in the area where some of the paint was chipped off the surface of the head.

Figure 5. A view of the fracture surface of the same rivet head in Figure 4. The white areas on the fracture surface (center area) and on the head shoulder (outer rim) are the corrosion products that had formed for a period of time before the head fell off the rivet shank.

Table 1. Composition of the Failed Aluminum Rivet Head Sample

Chemical Element	Sample (%)	Alloy 7277 (MIL-R-12221)[a] (%)
Iron	0.19	0.70 Max
Copper	1.23	0.80–1.70
Manganese	0.01	—
Chromium	0.21	0.18–0.35
Zinc	4.26	3.70–4.30
Titanium	0.04	0.10 Max
Silicon	ND	0.50 Max
Magnesium	ND	1.70–2.30
Aluminum	Remainder	Remainder

[a]U.S. Army Belvoir Research and Development Center. "Rivets, Solid, Aluminum Alloy 7277." MIL-R-12221D(ME), Fort Belvoir, VA, 25 Februry 1985.
ND = Not determined at this time.

and 7 are the microstructure of the rivet head containing a small secondary crack in the fracture. The crack was intergranular, indicating stress corrosion cracking (SCC). Apparently, high-pressure spraying with seawater to wash down the AVLBs from SWA had forced the seawater into crevices between the aluminum rivets and aluminum components of the bridge, particularly in the rivet holes. The trapped seawater that over a period of time caused corrosion that led to SCC in the rivet head. The initiation site for SCC occurred in the sharp head-to-shank fillet under the head shoulder that was formed as the result of cold head forming of the aluminum rivet by the rivet manufacturer. Alloy 7277 for the aluminum rivets used on the AVLB was susceptible to SCC in the presence of chloride ion in the corrosive environment involving seawater and salt-laden soil and dust as encountered by the bridge. Seawater may have accelerated corrosion on the aluminum rivets on the AVLBs that had been in service for a long time before being sent to SWA and then returned.

2.2 Metallurgical Evaluation of an Aluminum Rivet Sample With a Less Corrosion. In April 1994, a team composed of several personnel from Belvoir, TACOM, and ARL went to ANAD to evaluate the

Figure 6. As-polished microstructure of the failed aluminum rivet head showing a small secondary crack in the future. Magnification: 150×.

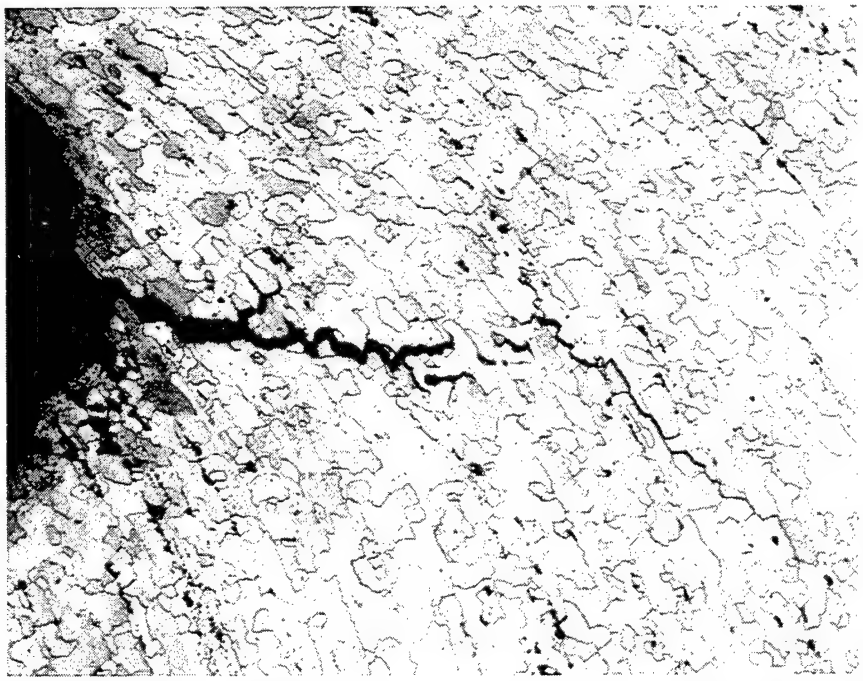

Figure 7. Etched microstructure of the same area in Figure 6 revealing that the crack is predominantly intergranular, indicative of stress corrosion cracking. The tail end of the crack had followed the grain flow formed as the result of the cold head-forming process by the rivet manufacturer. Magnification: 150×. Keller's etchant.

extent of corrosion on AVLBs from SWA. A hammer, chisel, and drift pin were taken along to the field, where the AVLBs were stored, to remove several aluminum rivets with their head still intact for further metallurgical evaluation. A number of rivet heads popped off the bridges when struck with the hammer only or with the chisel and hammer. Several heads were knocked off easily, and others did not, depending on the amount of cracking that had propagated during corrosion as seen on the surface of the fracture of the heads knocked off. In addition, there were a number of rivets with their head already fallen off on the AVLBs inspected at that time. In all cases, the heads that were knocked off as well as those that had fallen off broke at the head-to-shank fillet under the head. None of the driven ends of the aluminum rivets on the AVLBs inspected was observed to be missing or failed as the result of corrosion. A number of the failed rivets were in the bottom chords, forged center hinges, and forged connectors, where the primary stress will occur when heavy vehicles crosses the bridge. Attempts were made to drive the shanks of the failed headless aluminum rivets out of the rivet holes with the drift pin and hammer. Several rivet shanks came out, but not easily, depending on the amount of white deposits (corrosion products) already formed on the surfaces of the shank and rivet holes. There were other rivet shanks that could not be driven out because of volume build-up of extensive white deposits that binded the shank inside the rivet holes. The AVLBs would probably still function as long as the corroded rivets with cracked head and without the head stay in the rivet holes and the primary loads on the rivet shanks will be in shear rather than tension. In any event, there was no failure observed in the rivet shanks themselves that were driven out of the rivet holes.

One aluminum rivet with its head intact was removed from a forged aluminum center hinge of one AVLB from SWA at ANAD. This was done after the driven end of the rivet was cut off with the chisel and hammer. The rivet contained a small white deposit at the fillet (see Figure 8). There was no significant corrosion deposit on the rivet shank. The rivet was brought back to Belvoir for examination. Figures 9 and 10 are the microstructure of the area at the fillet containing the small white deposit. Integranular corrosion and cracks had already occurred in the corroded fillet, indicating SCC. Apparently, a small amount of moisture trapped in the crevice between the rivet and the components was enough to start corrosion. Given time, the cracks would have continued to propagate to the point that the rivet head would have fallen off or possibly been knocked off the shank, as did the failed rivets on the AVLBs from SWA at ANAD. In addition, the area in the fillet on the opposite side of the corroded area was not corroded and did not exhibit integranular corrosion or cracks.

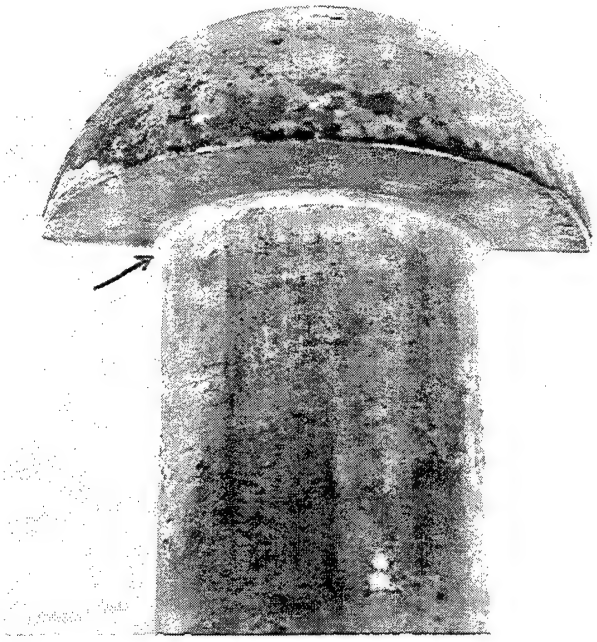

Figure 8. A view of a large aluminum rivet removed from a forged aluminum center hinge of one AVLB from SWA stored at ANAD. A small white corrosion deposit (arrow) can be seen in the head-to-shank fillet. A section of the head and shank with the corroded area was already cut off for microstructural examination. Magnification: 2×.

Figure 9. As-polished microstructure of the aluminum rivet in Figure 8. Integranular corrosion and cracks are present in the small corroded area in head-to-shank fillet, indicative of stress corrosion cracking. Magnification: 170×.

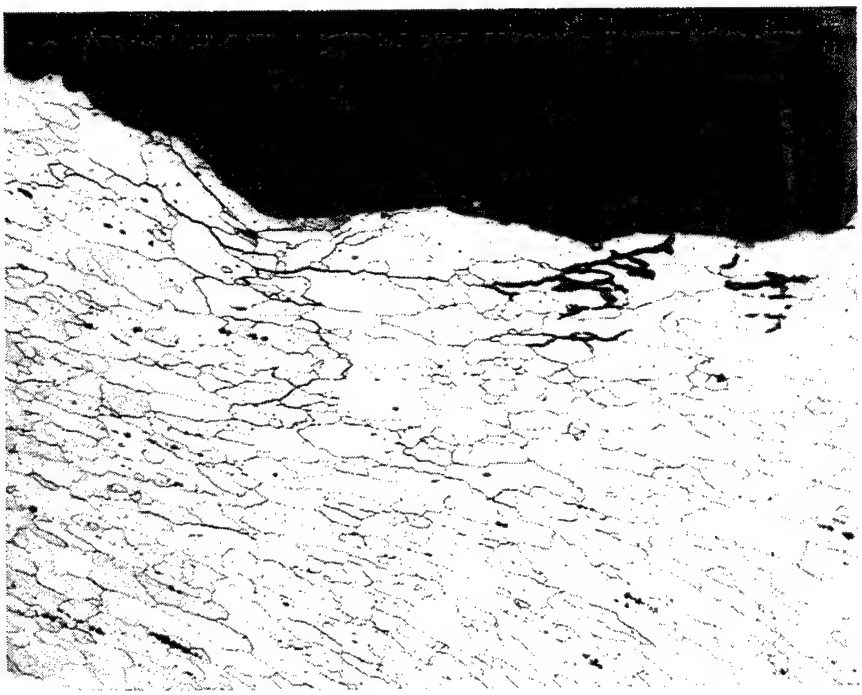

Figure 10. Etched microstructure of the same area in Figure 9. Magnification: 170×. Keller's etchant.

2.3 Metallurgical Examination of Several Corroded AVLB Aluminum Component Samples. A number of corroded aluminum component samples along with several corroded aluminum rivets were received from ANAD for examination. They were removed from an AVLB center panel assembly thatwas dismantled at ANAD in order to determine the extent of corrosion. Figure 11 shows a section of a top chord angle containing a corroded hole, caused by exfoliation, near a countersunk rivet hole. The corroded hole was located on the exposed surface of the angle at the space (gap) between two extruded aluminum tread decks that were bolted side-by-side on top of the angle chord. It was speculated that the debris, such as dirt, was trapped in the space and was in contact with the exposed surface of the angle. With the debris being wet from the weather and/or seawater, exfoliation corrosion took place there and, after a period of time, even extended laterally to the rivet hole (see Figures 11–13). Alloy 2014 used for aluminum structural angle was susceptible to exfoliation under corrosive environments encountered by the AVLBs.

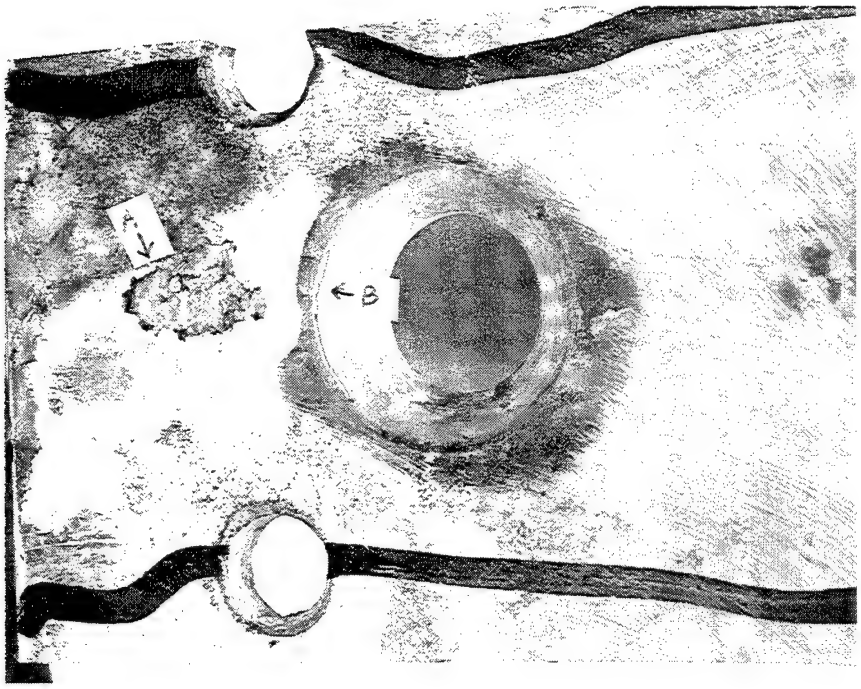

Figure 11. Large corroded hole (A) on top surface of the top chord angle section cut from AVLB center panel dismantled at ANAD. Exfoliation had extended laterally beyond the hole of the corroded area. Delaminated surface crack (B) due to exfoliation was observed near the top of the large countersunk rivet hole. Slightly larger than actual size.

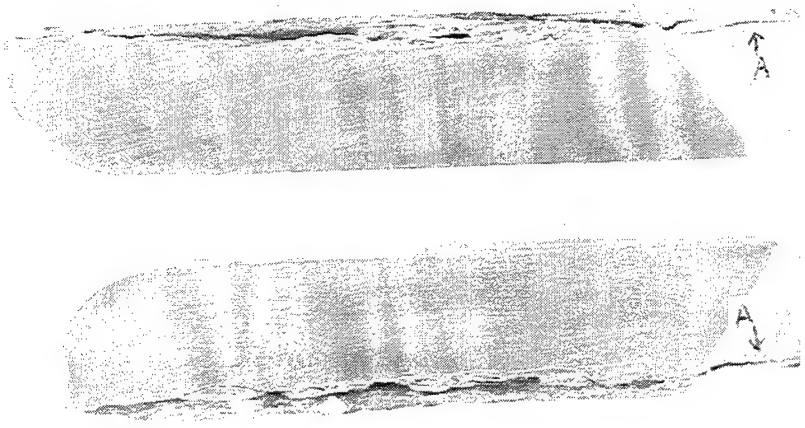

Figure 12. Matched half sections of the corroded sample in Figure 11. It was cut in two through the large corroded hole. Delaminated surface cracks (A) were observed in the countersunk section of the rivet hole on the right, revealing extensive exfoliation beyond the corroded hole. Magnification: approximately 2×.

Figure 13. As-polished microstructure at the bottom of the corroded hole in Figure 11. Exfoliation was the primary mode of corrosion on the corroded surface of the angle section of the AVLB top chord. Magnification: 75×.

Another sample examined was the corroded aluminum rivet with its one end still in a rivet hole of an aluminum spacer bar (see Figures 14 and 15). Both rivet shank and spacer bar were heavily covered with white corrosion products. Figure 16 shows the microstructure containing small corrosion pittings in the surface of the corroded rivet shank in the rivet hole. Small cracks had initiated from the bottom of the pits.

A 4-in-long corroded aluminum rivet sample with heavy white corrosion deposits on the surface of its shank also was examined (see Figure 17). Figures 18 and 19 are the microstructure of a corroded area on the shank surface. Intergranular corrosion and cracks were present on the corroded surface.

2.4 Shear Tests of Six AVLB Aluminum Rivet Samples. Many aluminum buttonhead rivets were removed from several AVLBs from SWA at ANAD to determine the extent of the rivet corrosion and damage. A number of them were used by the laboratory personnel at ANAD to establish the procedure to inspect the rivet heads for cracks by ultrasonic method. So far, extensive damage by corrosion was restricted to SCC in the head-to-shank fillet under the head, in some cases resulting in complete head

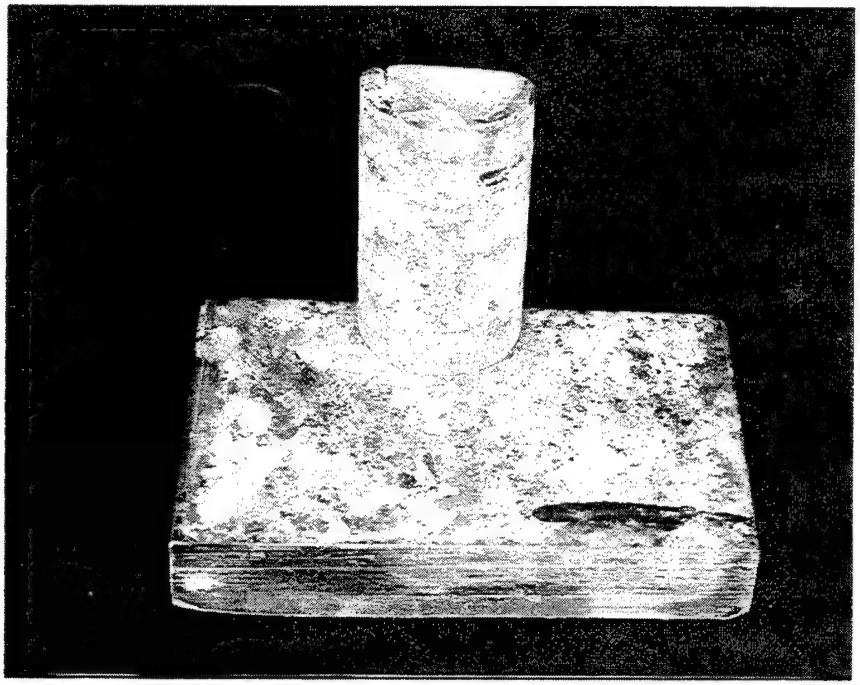

Figure 14. A section of the aluminum rivet shank still in the rivet hole of the spacer bar removed from the AVLB center panel assembly dismantled at ANAD. The bare surfaces of the rivet and bar were heavily covered with the white corrosion products. This sample was already cut in two for metallurgical examination. Magnification: approximately 1.25×.

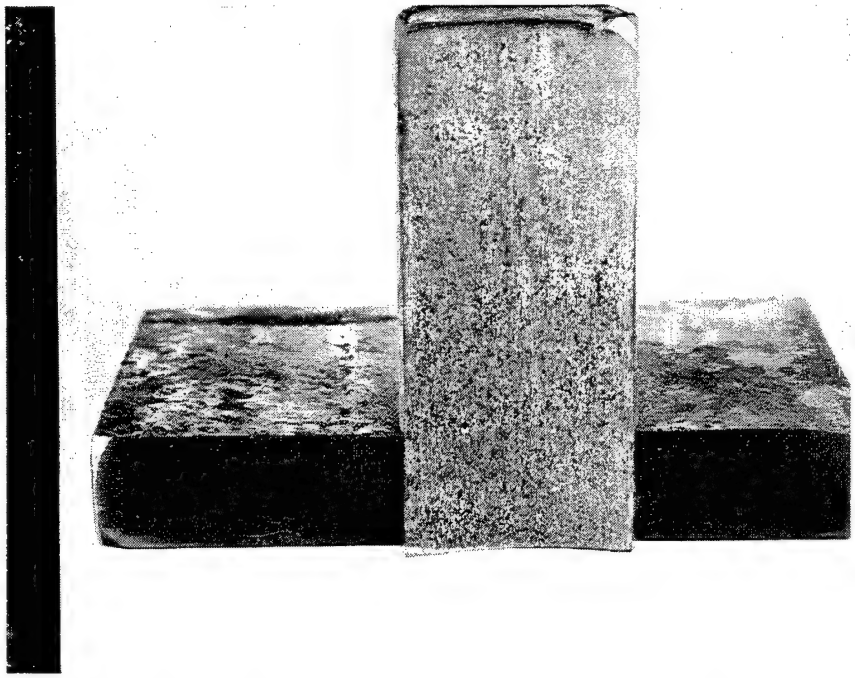

Figure 15. Etched cross section of the sample in Figure 14 to show end of the rivet shank still in the rivet hole of the spacer bar. Magnification: approximately 1.6×. Keller's etchant.

Figure 16. As-polished microstructure of the rivet shank (right) and space bar at the interface in the rivet hole of the bar in Figure 15. Small corrosion pitting had occurred on the shank surface of the rivet in the rivet hole of the bar, resulting in small cracks initiating from the bottom of the pits. Magnification: 190×.

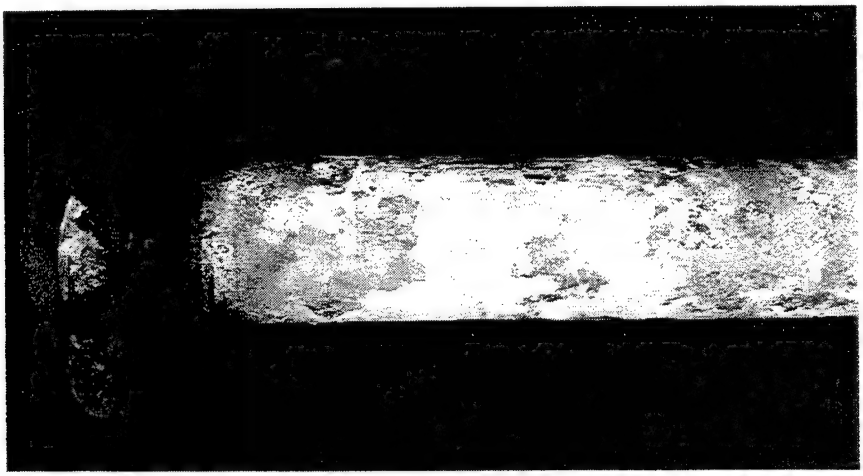

Figure 17. A 4-in-long large aluminum rivet sample with heavy deposits of white corrosion products on the surface of its shank. The driven end of the rivet is on left. Slightly larger than actual size.

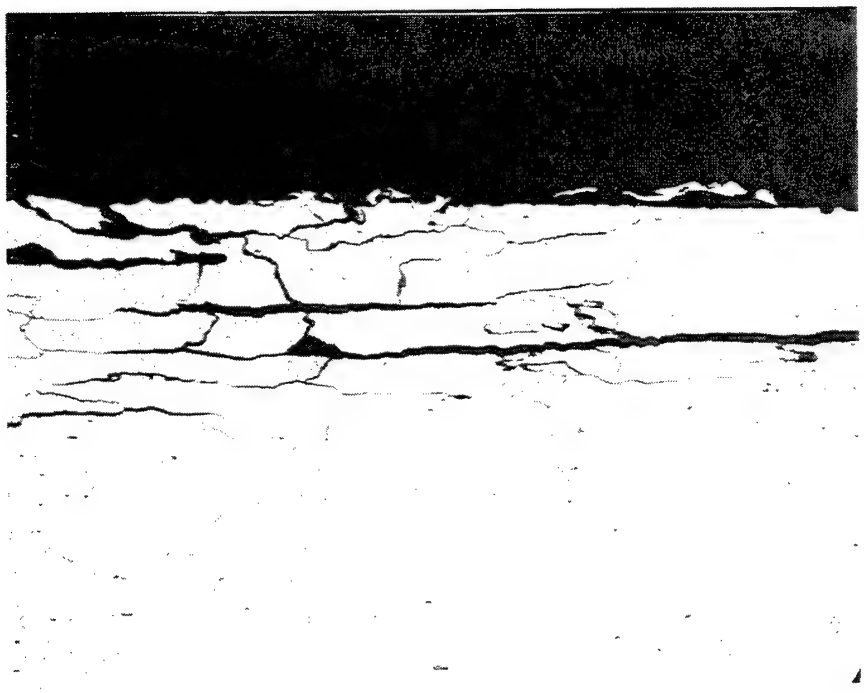

Figure 18. As-polished microstructure of a small corroded area on the surface of the rivet shank in Figure 17 covered with thick corrosion products. Integranular corrosion and cracks (SCC) were observed at the corroded surface. Magnification: 100×.

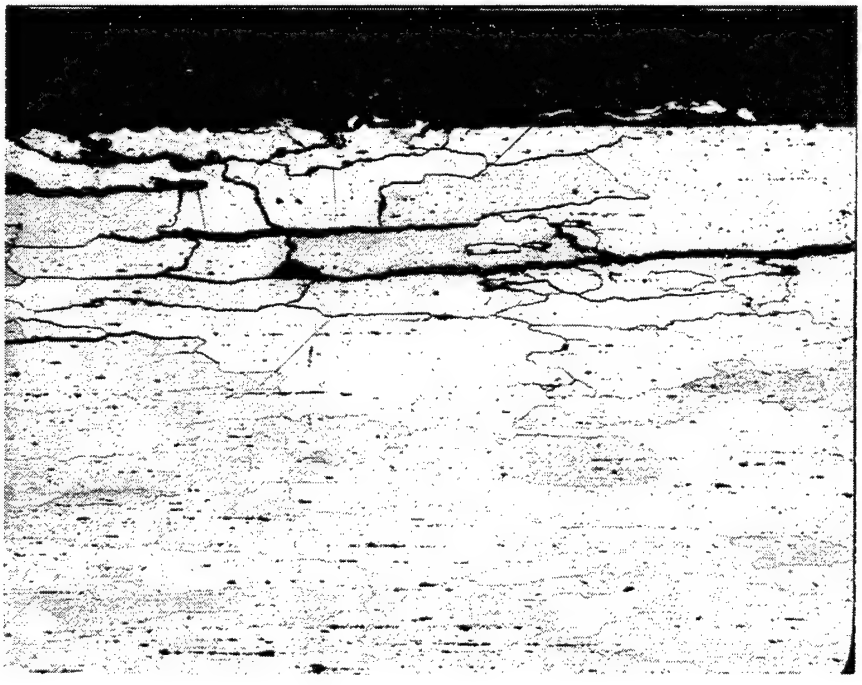

Figure 19. Etched microstructure of the same area in Figure 8. Magnification: 100×. Keller's etchant.

failure, with the head falling off. There was no reported failure in the corroded rivet shanks by cracking. A concern was raised regarding the integrity of the shank of the corroded rivets with the cracks in the head or after the head had fallen off and with the corroded rivet shank still remaining in the rivet holes.

Six small aluminum angle chord sections, with each containing an aluminum rivet holding together two 5-in structural angles and an aluminum girder plate in between them, were received from ANAD for the shear tests. Based on the ultrasonic inspection performed on the rivets at ANAD, three of them were marked "Good" and the other three as "Corrosion Cracked." Figures 20 and 21 show the shear test specimens with the rivet in the low and high position on the vertical leg of the angles, respectively.

A typical setup of the test specimen for the shear test on the testing machine is shown in Figure 22. Two clamps were used, one above and the other below the rivet, to prevent both angle vertical legs from spreading apart during the test. The girder plate with the protruded end at the top served as the plunger to shear the rivet shank in the rivet holes. This setup simulated the loading of the rivet shank by shear as will occur on the rivets installed on the AVLBs bottom chords and forged center hinges where the primary concerns are addressed on the integrity of the corroded rivets.

A deflectometer was used in order to obtain a load-deflection curve for each specimen. The load was applied in compression on the protruded end of the girder plate plunger between the angles until double shearing occurred on the rivet shank in the rivet holes. The results of the shear tests on six AVLB aluminum rivet samples are given in Table 2. The shear strengths obtained for the tested rivets ranged from 46,600 to 49,000 psi (or maximum load to shear, 44,000 to 46,000 lb), indicating no significant difference in the shear strengths among the "Bad" and "Good" rivets.

Figure 23 shows the enlarged crack in the head-to-shank fillet under the head of a "Bad" rivet sample after the shear test. Cross sections of the "Bad" rivet head with the cracks and the "Good" rivet head with no cracks are shown in Figure 24. A large crack can be seen initiating at the sharp fillet with the path of the small crack following the grain flow formed as the result of cold head forming by the rivet manufacturer. In all cases, white deposits of the corrosion products were observed on the surfaces of the shanks of all rivets and in all rivet holes.

When the load-deflection curves were reviewed, each curve began to deviate from the straight line at about 30,000 lb. This would indicate permanent deformation of the test specimen, primarily in the rivet hole of the girder plate plunger and in the shank of the rivet (see Figure 25).

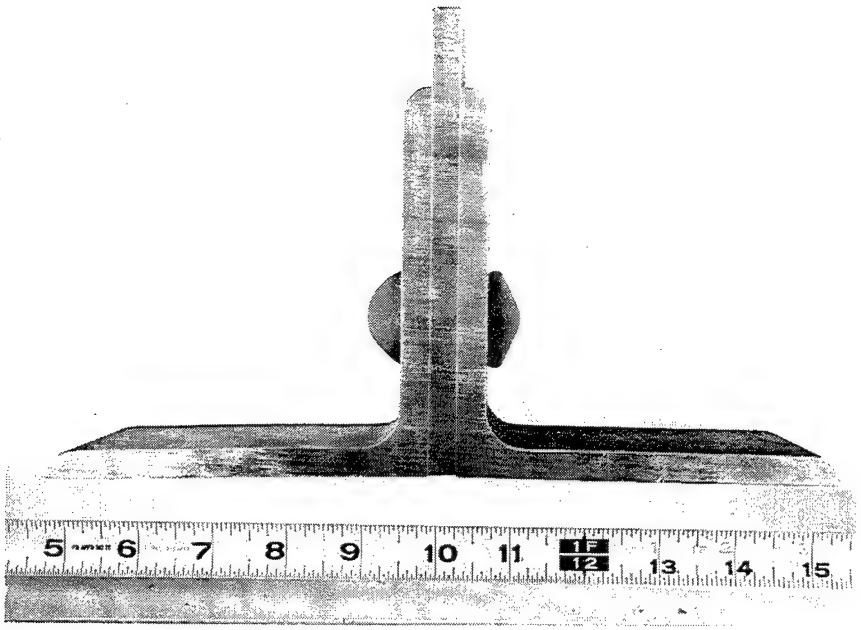

Figure 20. A shear aluminum test specimen cut from AVLB panel assembly, showing the rivet at the low position. The specimen was composed of two angles with the middle girder plate to serve as a plunger to shear the rivet.

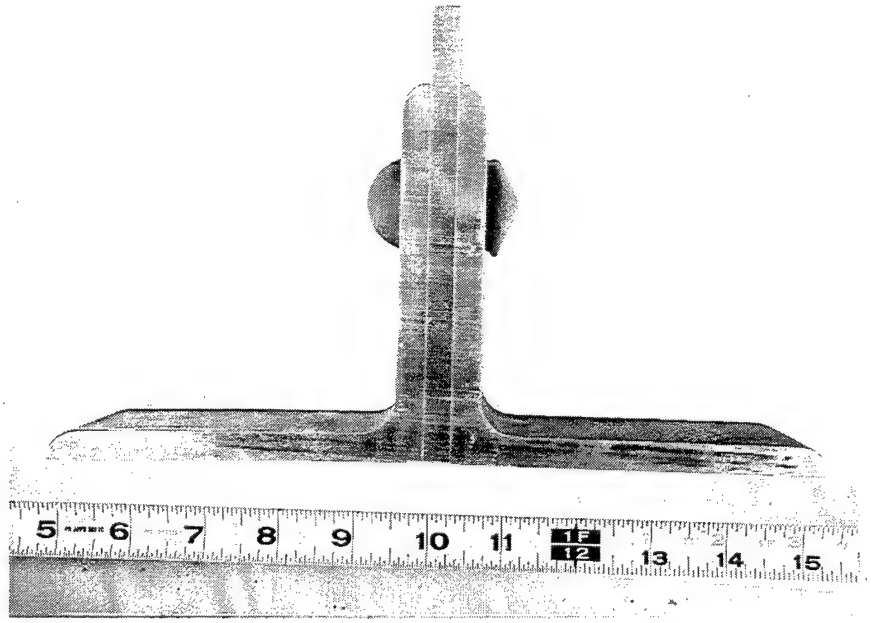

Figure 21. A shear aluminum test specimen showing the rivet at the high position.

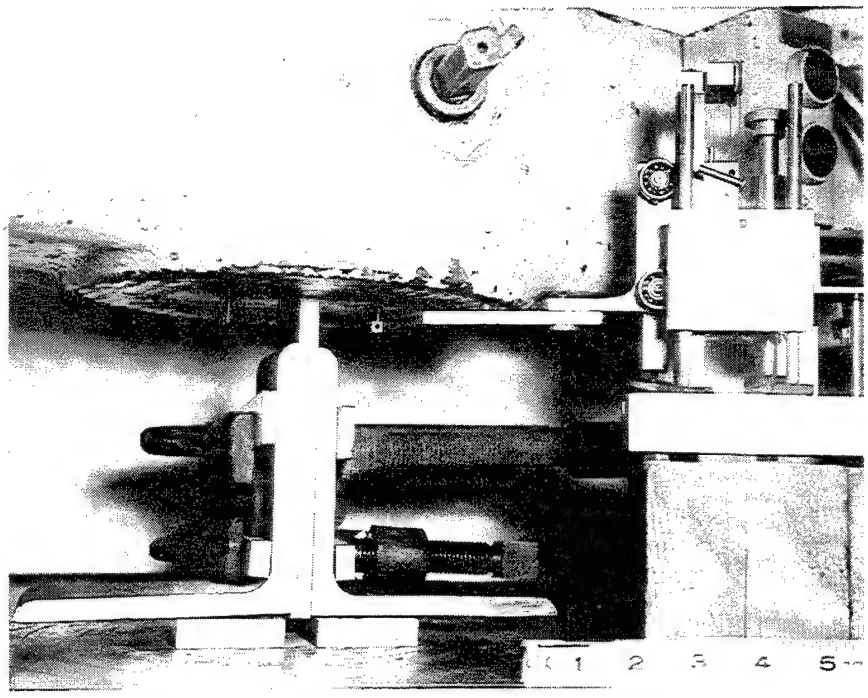

Figure 22. A typical setup of the AVLB rivet shear test specimen on the testing machine for double shearing of the rivet shank. The clamps were used above and below the rivet to prevent both angle vertical legs from spreading apart during the test. The test specimen sat on top of two 0.5-in-thick aluminum blocks to allow the bottom of the girder plate plunger to extend beyond the bottom of the angle horizontal legs during the test. The load was applied in compression to the protruded top of the specimen plunger under the compression head in the cross head of the testing machine. A deflectometer was used to measure the movement of plunger to obtain load-deflection curve.

Table 2. Shear Property of Six AVLB Corroded Rivet Specimens

Specimen	Position of Rivet	Maximum Load to Shear (lb)	Shear Strength (psi)
1 Bad	High	43,950	46,580
2 Bad	Low	45,350	48,070
3 Bad	High	44,050	46,690
4 Good	Low	46,250	49,020
5 Good	Low	45,350	48,070
6 Good	High	44,900	47,591

Note: Approximate diameter of hot-driven rivet is 0.775 in.

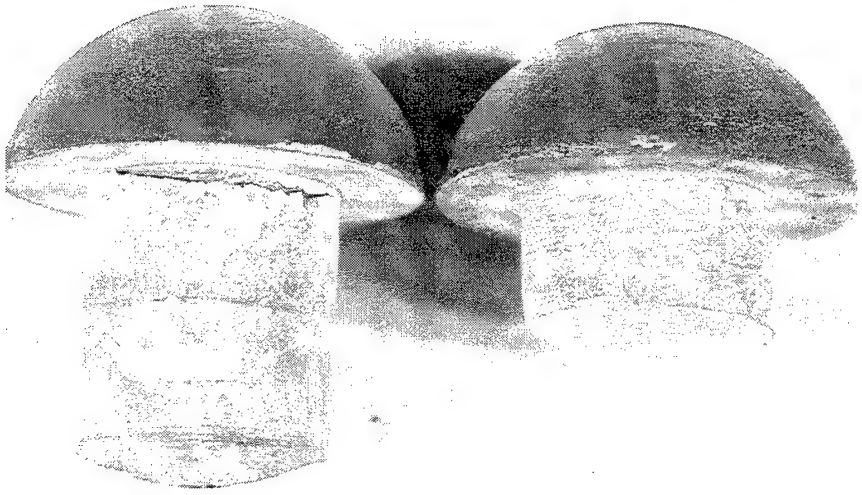

Figure 23. View of "Bad" (left) and "Good" rivets after the shear tests. A large crack is seen in the head-to-shank fillet of the "Bad" rivet. White corrosion products were on the surface of the rivet shank of both rivets. Magnification: approximately 1.33×.

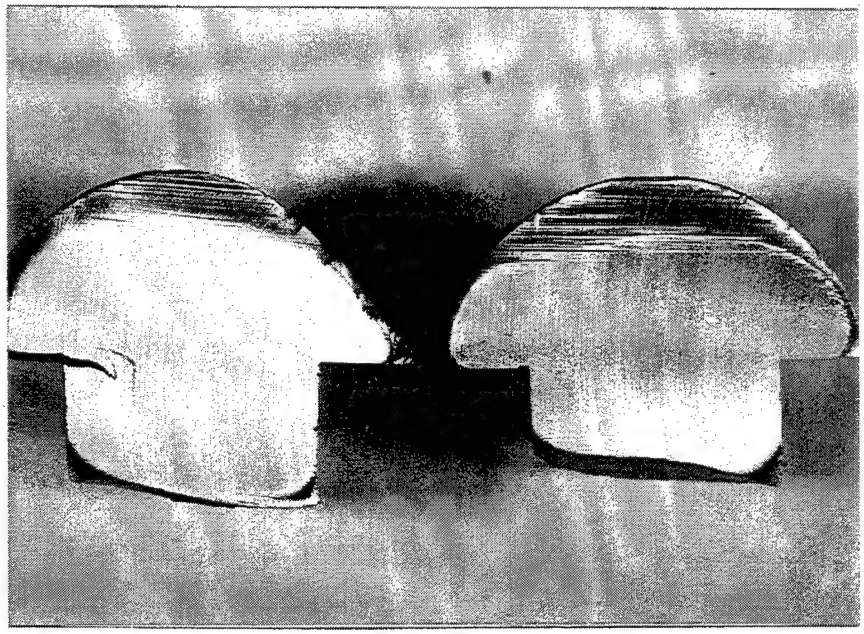

Figure 24. Cross sections of AVLB corroded rivet heads sectioned in two after the shear tests. The "Bad" rivet with large and small cracks in the left fillet under the head on the left. The "Good" rivet on right did not have observable cracks. Magnification: approximately 1.33×. Grit 600 surface finish.

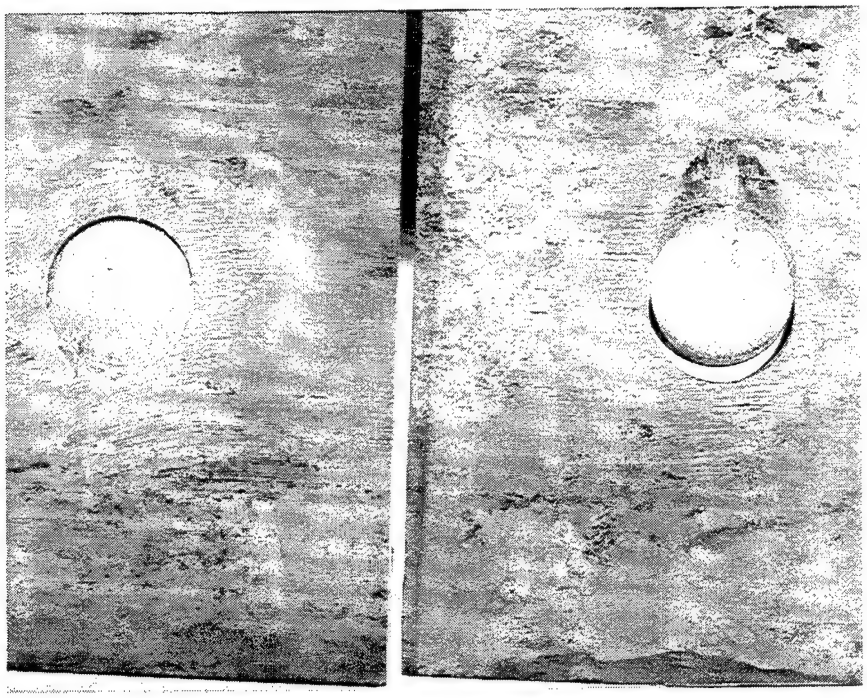

Figure 25. View of the rivet holes in the angle vertical leg on left and in the girder plate plunger on right after the shear test. Elongation of the rivet hole in the plate plunger was greater than the hole in the angle leg as noted by the gap. Sheared sections of the rivet shank remained in the holes. Actual size.

2.5 Mechanical Properties of Several Aluminum Alloy 7277 Rivet Samples. In order to determine their mechanical properties, the following 0.75-in-diameter aluminum alloy 7277 rivet samples were obtained and tested:

- Specimen A: A 4-in-long hot-driven buttonhead rivet removed from an AVLB at ANAD.
- Specimen B: A 6-in-long hot-driven buttonhead rivet removed from an AVLB at ANAD.
- Specimen C: New 8-in-long buttonhead rivet in as-received condition from ANAD.
- Specimen D: New 8-in-long countersunk flat head rivet in as-received condition from ANAD.

In addition to the tension and shear tests, Brinell hardness tests were conducted on the samples after the tests. The shear tests were performed on the new rivet sample after the tension tests in the same

manner as were done previously for the AVLB corroded hot-driven aluminum rivets (see shear tests of six AVLB aluminum rivet samples in section 2.4 of this report). The aluminum angles with the rivet holes were reused from the previous shear tests. A new plunger with a rivet hole was used to shear each rivet sample.

The results of the mechanical tests on the aluminum alloy 7277 rivet samples are given in Table 3. The new rivets (specimens C and D) met the minimum tensile and shear strengths specified in ASTM B 316 or Military Specification MIL-R-12226 for alloy 7277 in T62 temper condition. Alloy 7277 rivets are hot-driven at an elevated temperature to increase their driving characteristics, and their high-shear strength is developed by natural aging after hot driving as indicated by the shear tests done previously on the AVLB corroded rivets (47,670 psi vs. 37,645 psi for the new, not hot-driven rivets). Although hot driving at the elevated temperature will destroy the original tensile properties in T62 temper condition of the as-received new rivets, their properties will be restored by natural aging as indicated by specimens A and B after they were hot-driven on the AVLB and naturally aged for several years.

Table 3. Mechanical Properties of Aluminum Alloy 7277 Rivet Samples[a]

Specimen	Tensile Strength (psi)	0.2% Offset Yield Strength (psi)	Elongation (%)	Shear Strength (psi)	Brinell Hardness (HB)[b]
A	70,360	50,110	21.0	—	119
B	70,170	50,930	21.5	—	119
C	68,110	44,730	24.3	38,710[c]	109
D	66,470	40,530	24.8	36,580[c]	105
ASTM B 316 and MIL-R-12221 for alloy 7277-T62					
	60,000 min.			35,000 min.	
AVLB corroded hot-driven rivets					
				47,670 (average for six samples)	

[a] Specimen A was subsize 0.25-in-diameter round tension test specimen with 1-in gauge length, whereas specimens B, C, and D were standard 0.5-in-diameter round tension test specimens with 2-in gauge length.
[b] Brinell hardness test (10-mm-diameter steel ball and 500-kg load for 30 s).
[c] Shear tests were done on the grip ends of specimens C and D after the tension tests.

2.6 Clamping and Breaking Loads of Six Installed Aluminum Rivets From AVLB. In order to determine the clamping and breaking loads of the installed (hot driven) 0.75-in-diameter aluminum alloy 7277 rivets on AVLB, two test methods were used. For the first method, approximate clamping load was determined by measuring the change in the length of the rivet before and after the center aluminum girder plate was removed from between two 5-in aluminum structural angles as seen in Figure 20. For the second method, a special pull test was set up in such a manner that an installed rivet was loaded in tension during the test until a failure occurred.

A large section containing at least six installed rivets was cut from the top angle chord of the AVLB female center panel assembly in Belvoir. From this large section, six 3-in-wide test specimens, each containing a rivet holding two angles and a center girder plate together, were cut for the tests. In order to perform the special pull test on the rivet of the test specimen, three 0.5-in-diameter holes were drilled 120° apart around one rivet end through two 0.375-in-thick plates (an angle vertical leg and a girder plate) on one side of the specimen (see Figure 26). Then three more similar holes rotated 60° were drilled around the other rivet end through the opposite side of the same specimen. Two-in-long, 0.5-in-diameter steel dowel pins were inserted in those holes (three on each side, see Figure 27). In this manner when the compression load was applied on those pins, the rivet was pulled apart in tension until it failed (see sketch in Figure 28).

Before the pull test of each specimen was performed, a small center punch hole was made on each end of each rivet (one on the manufactured head and the other on the driven end). This was done to facilitate the measuring of the rivet length when using a micrometer (capable of reading 0.0001-in divisions) with a 0.25-in-diameter steel ball on each anvil). Measurements of the rivet length were performed before and after the center girder plate was removed from the specimen prior to the pull test. To facilitate the removal of the center plate from the test specimen, a 0.375-in-diameter hole was drilled into the edge of the plate to the depth just above the rivet shank. A similar hole was drilled into the opposite plate edge in the same manner. The plate was removed in the testing machine by breaking it in two pieces at the drilled edge holes and sliding both of them out from between the two angle legs. The approximate clamping load for each rivet specimen was calculated based on the change in the rivet length measured.

The results of the pull tests and clamping load determinations for six AVLB rivet specimens are given in Table 4. All rivet specimens except specimen D broke at the fillet under the rivet head to various

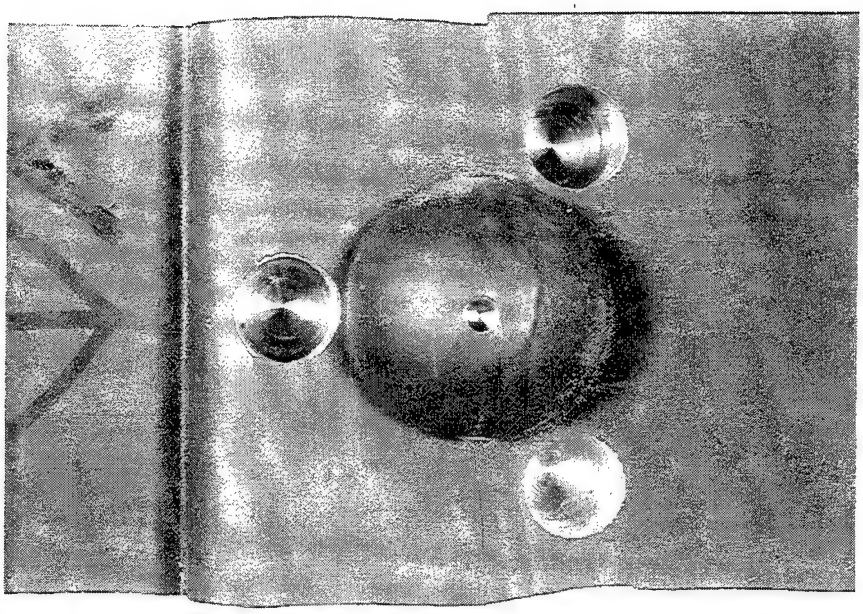

Figure 26. Typical pull test specimen with three 0.5-in-diameter holes drilled 120° apart around the rivet head on one side of the specimen. A center punch hole or a small drill pilot hole was made on the end of the head as on the driven end of the rivet to facilitate measuring of the length of the rivet using a micrometer. Actual size.

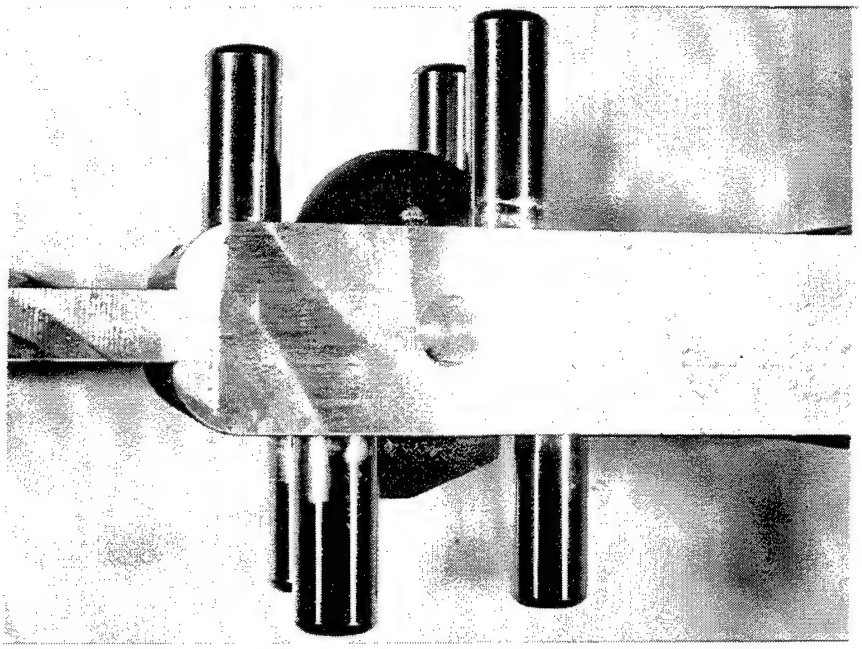

Figure 27. Side view of the pull test specimen with the 0.5-in-diameter steel dowel pins already inserted in the drilled holes of the angle legs and girder plates. Note the 0.375-in-diameter hole drilled into the edge of the girder plate, which will be removed prior to the pull test. Actual size.

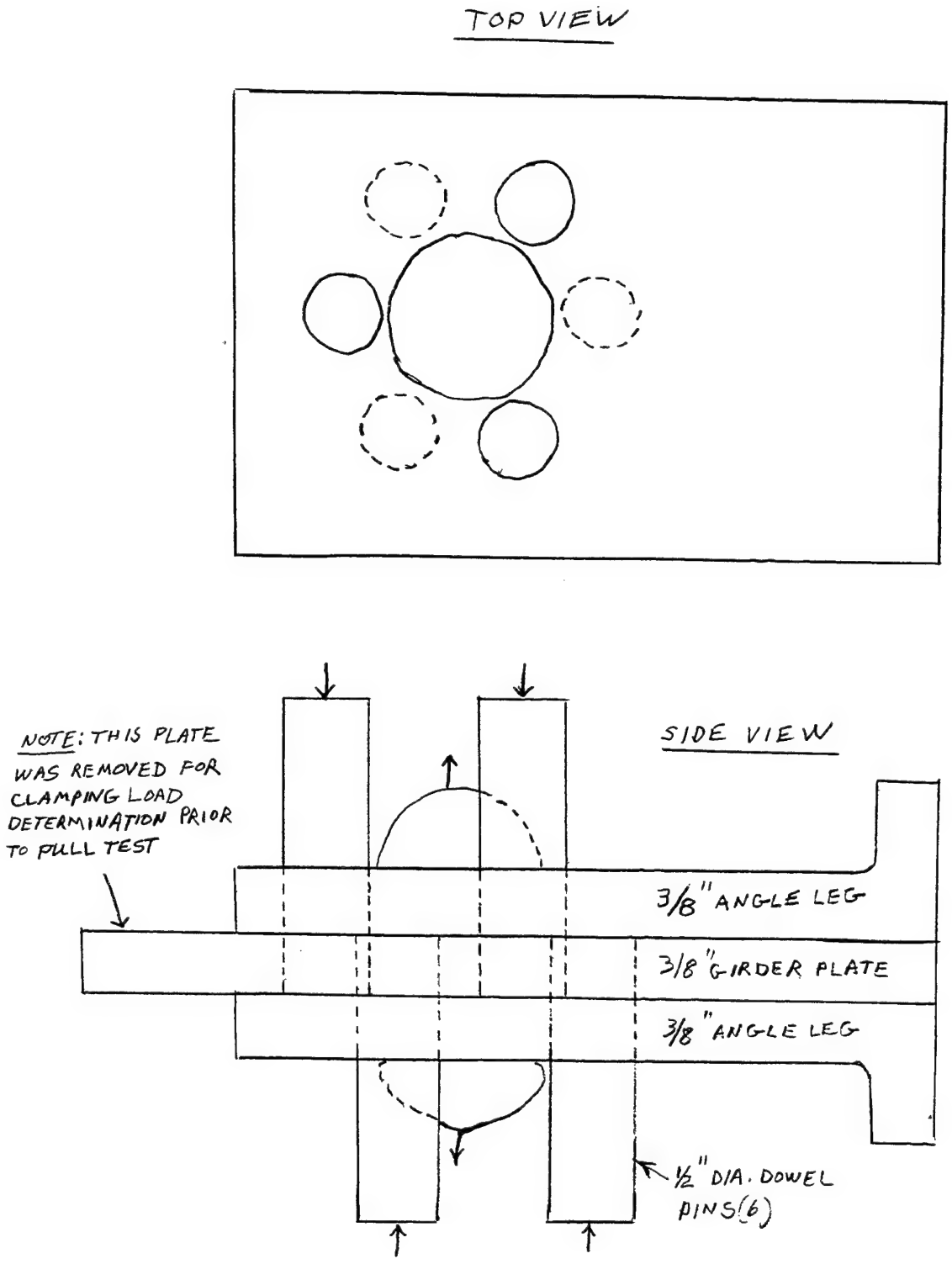

Figure 28. Sketch of pull tests to pull the rivet in tension by applying compression load on the dowel pins (top and bottom view).

Table 4. Clamping and Breaking Loads of Six AVLB Rivet Specimens

I. APPROXIMATE CLAMPING LOAD DETERMINATION BY CALCULATION				
Specimen	Difference[a] (in)	Strain[b] (in/in)	Stress[c] (psi)	Clamping Load[d] (lb)
A (high)	0.0015	0.00133	13,670	6,450
B (low)	0.0012	0.00107	10,930	5,160
C (high)	0.0017	0.00151	15,490	7,310
D (low)	0.0014	0.00124	12,760	6,020
E (high)	0.0016	0.00142	14,580	6,880
F (low)	0.0016	0.00142	14,580	6,880
II. BREAKING LOAD BY THE PULL TESTS				
Specimen	Breaking Loads (lb)	Tensile Strength[e] (psi)	Remarks[f]	
A	29,550	62,640	Prior Cracks	
B	22,500	47,700	Prior Cracks	
C	25,800	54,690	Prior Cracks	
D	32,750	Sheared in the driven end	Prior Cracks	
E	21,850	46,320	Prior Cracks	
F	23,350	49,500	Prior Cracks	

NOTE: "High" and "low" refer to the position of the rivet holes on the angle vertical legs.

[a] The difference in lengths of the rivet (end to end) before and after the removal of the center girder plate.

[b] Based on the grip length in the shank of the rivet holding two angles and girder plates together: 1.128 in.

[c] E = 10,250,000 psi as the approximate modulus of elasticity for alloy 7277 for stress determination: stress = E × strain.

[d] Clamping load = stress × area where area equals 0.4717 in^2 for 0.775-in diameter of the rivet shank of the test specimens.

[e] Cross-sectional area of 0.4717 in^2 based on 0.775-in diameter was use for calculating the stress.

[f] White corrosion products observed on the rivet shank and holes. The amounts of discoloration from corrosion in the prior cracks varied from specimen to specimen.

extent because of prior cracks (see Figure 29 for an example) that were observed in the fracture surface as a discoloration from corrosion (stress corrosion cracking). This was confirmed by the white corrosion products observed on the surfaces of the rivet shank and of the rivet holes in both angles and the center girder plate. Depending on the extent of cracks from corrosion, the breaking loads of the installed rivets varied from 21,850 to 29,550 lb. Specimen D rivet failed by shearing at the driven end (see Figure 30)

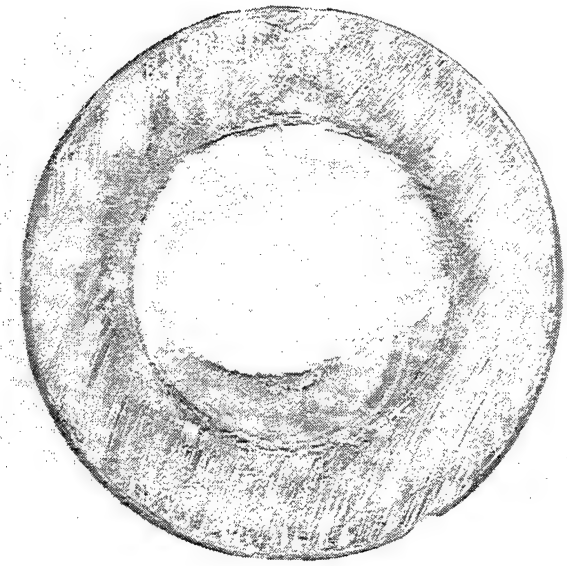

Figure 29. Enlarged view of the fracture surface of the rivet head (specimen C) that broke at the head-to-shoulder fillet after the pull test, revealing the darkened area of the crack because of corrosion (stress corrosion cracking).

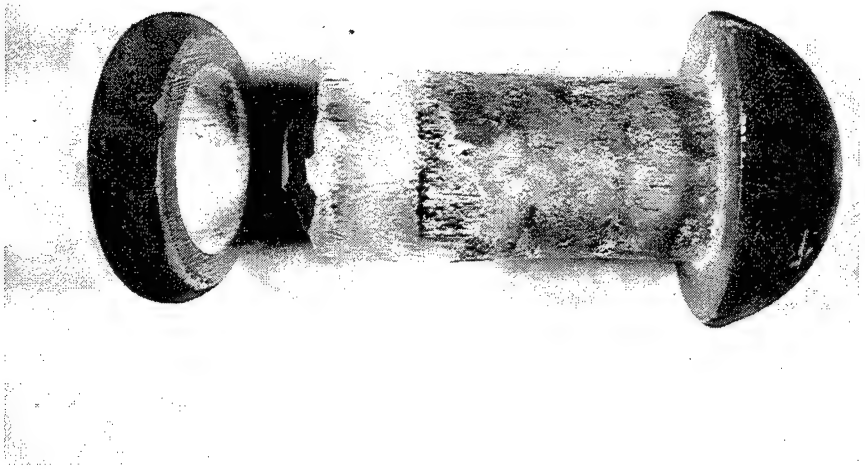

Figure 30. A view of the rivet (specimen D) with the sheared driven end (left) after the pull test.

at 32,250 lb. The approximate clamping loads determined for the installed rivets by calculation varied from 5,160 to 7,310 lb. Some strain relaxation may have occurred due to cracking in the rivet head, as revealed by the pull tests and presence of the corrosion products on the rivet shanks and holes.

Figure 31 shows a cross section of another installed rivet that was cut from the same large section mentioned previously but not used in the test. Large and small cracks were observed in the rivet head, initiating at the fillet. This confirmed the finding that all rivet specimens tested, except specimen D, did contain prior cracks because of corrosion. In addition, Figures 32 and 33 show the cross section of a rivet sample removed elsewhere (top connector) on the same AVLB in Belvoir, again revealing the cracks in the rivet head as the result of the corrosion.

2.7 Pull Tests on Two New AVLB Installed Aluminum Rivet Specimens. A similar pull test as described previously was performed on two newly installed 0.75-in-diameter aluminum alloy 7277 rivets in the angle chord section cut from AVLB in order to determine their breaking load. In this case, the old rivets were removed one at a time and replaced with new rivets that were heated to 1,020° F and then hot-driven, holding two 5-in aluminum angles and a girder plate in between together. Holes were drilled in both riveted test specimens as usual so that the rivet itself was loaded in tension to failure.

The results of the pull tests on two new rivet test specimens are given in Table 5. Their breaking loads were higher than the previous five rivets that contained cracks in their head from corrosion.

2.8 Tests on Two "Good" and Two "Bad" AVLB Rivet Specimens. Pull and shear tests were performed on four installed AVLB aluminum rivet specimens submitted by ANAD. Based on the ultrasonic inspection done at ANAD, two of them were labeled as "Good" and the other two as "Bad." In addition, approximate clamping loads were determined for the rivets.

The information on the four rivet samples removed from two AVLB female center panels (FSN 5420-00-542-3115) is given in Table 6. Each specimen was an angle chord section containing a 0.75-in-diameter rivet holding together two 5-in aluminum structural with an aluminum girder plate between them (similar to Figure 20). During the preparation of the rivet specimens for the tests, portions of the manufactured rivet head and driven end were inadvertently cut off of specimen D (see Figure 34). The clamping load determinations, pull tests, and shear tests were performed in the same manner as described earlier in this report. With one slight exception, a small pilot hole, in lieu of a center punch hole, was

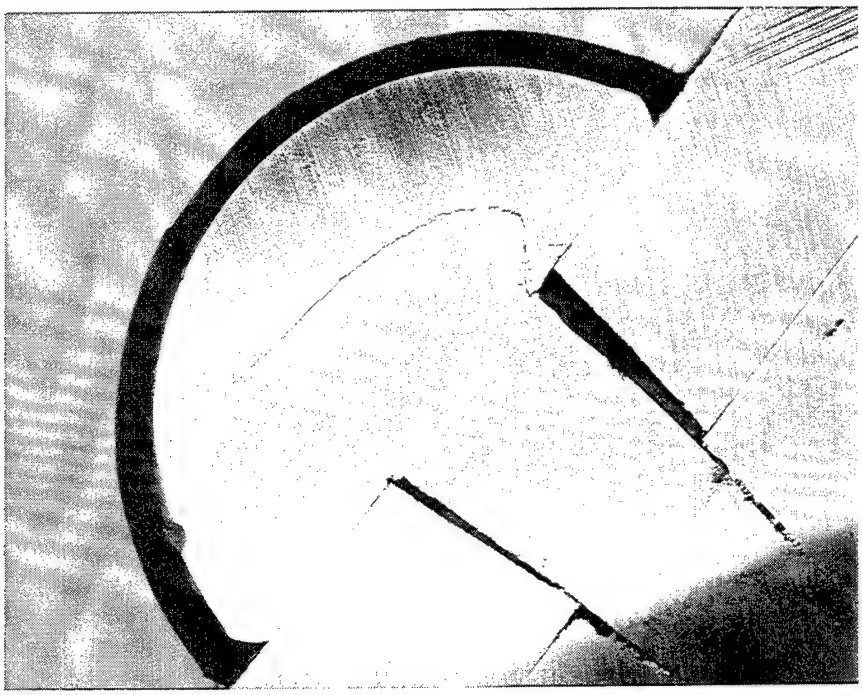

Figure 31. A view of the cross section of the installed rivet showing a large crack in the head. The crack initiated in the fillet. Magnification: 3×. As-polished.

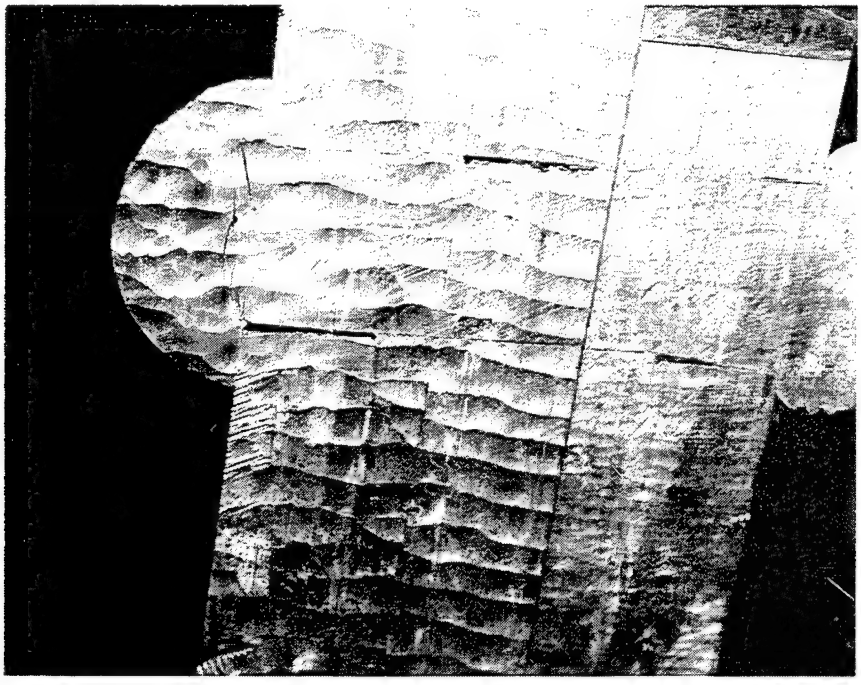

Figure 32. A view of the rivet that was rough cut in half lengthwise in the top connector of the AVLB, thus revealing large cracks in the head. The crack initiated in the filiet. See Figure 33 for polished surface of the same rivet.

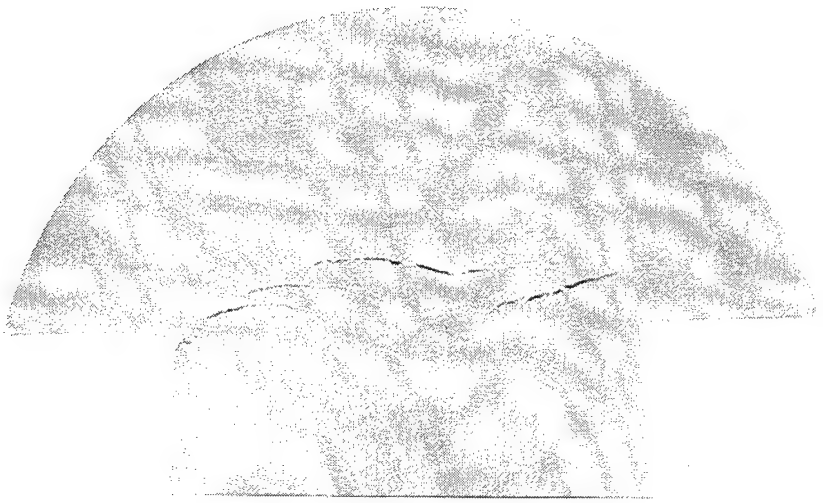

Figure 33. Same rivet in Figure 32, except with as-polished surface of the cut areas.

Table 5. Breaking Loads of New Aluminum Rivets by Pull Tests

Specimen	Breaking Load (lb)	Tensile Strength (psi)	Remarks
1	30,650	64,974	Broke at head-to-shank fillet.
2	32,600	69,107	Broke in middle of rivet shank.

Table 6. Description of Aluminum Rivet Samples for AVLB Female Center Panel

Specimen	Status	Angle Chord	Rivet Hole Position	Contract No.
A	Good	Bottom	High	P088CD50978LA
B	Good	Top	Low	PO88CD50978LA
C	Bad	Bottom	High	DAAK01-70-C-3307
D	Bad	Top	Low	DAAK01-70-C-3307

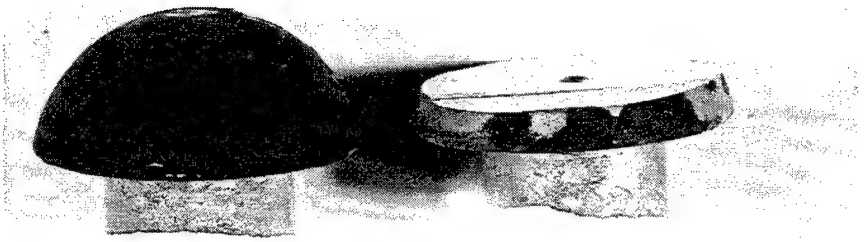

Figure 34. A view of two rivet heads (specimen B on left and specimen D on right) after the shear tests. A portion of specimen D rivet head was inadvertently cut off during the specimen preparation prior to the pull and shear tests.

drilled in each end of the rivet to facilitate measuring of the length of the installed rivet with a micrometer. The sample rivet specimens were used in all tests: first the clamping load determination, next the pull test, and finally the shear test. In addition, an ultrasonic inspection was conducted on the rivets prior to the tests.

The results of the clamping load determination, pull tests, and shear tests on the "Good" and "Bad" AVLB rivet specimens from ANAD are given in Table 7. The approximate clamping loads determined varied from 5,170 to 8,600 for rivet specimens A, B, and C. Instead of breaking during the pull tests, specimens A and B (both "Good") failed by shearing from their driven end through the rivet hole of the angle leg (see Figure 35). The approximate shear strengths were calculated to be 39,360 and 38,170 psi for specimens A and B, respectively. The breaking shear load for both rivets was about 31,000 lb. Specimen C (the "Bad" rivet) broke at 15,000 lb at the head-to-shank fillet during the pull test. Figure 36 shows the extent of the crack, because of corrosion, observed on the fracture surface of specimen C after the test. Approximately 65% of the discolored area in the fracture was associated with the crack because of SCC. This explained the reason for the low breaking load recorded for the "Bad" rivet as compared

Table 7. Test Results on "Good" and "Bad" ALVB Rivet Specimens

I. APPROXIMATE CLAMPING LOAD DETERMINATION			
Specimen	Strain[a] (in/in)	Clamping Load (lb)	
A "Good"	0.00142	6,870	
B "Good"	0.00107	5,170	
C "Bad"	0.00178	8,600	
D "Bad"	Not Determined	—	
II. PULL TEST			
Specimen	Breaking Load (lb)	Shear Strength[b] (psi)	Remarks
A "Good"	31,000	39,360	Sheared in driven end.
B "Good"	30,700	38,170	Sheared in driven end.
C "Bad"	15,300	—	Head broke off, 32,430-psi tensile strength.
D "Bad"	Not determined	—	—
III. SHEAR TEST			
Specimen	Diameter (in)	Shear Load (lb)	Shear Strength (psi)
A "Good"	0.767	39,600	42,850
B "Good"	0.770	40,000	42,950
C "Bad"	0.760	33,850	37,310
D "Bad"	0.750	34,600	39,160

[a] Strain is based on the grip length of the rivet: 1.125 in.

[b] Shear strength is based on measuring approximate sheared area of the sheared end of specimens A and B.

to the much higher loads obtained for the "Good" rivets. Thick layers of the white corrosion products were observed on the surfaces of two angle vertical legs and the girder plate in contact with each other in both "Bad" specimens. This was indicative of extensive corrosion in the angle chord areas of the AVLB for a period of time under certain corrosive environmental conditions.

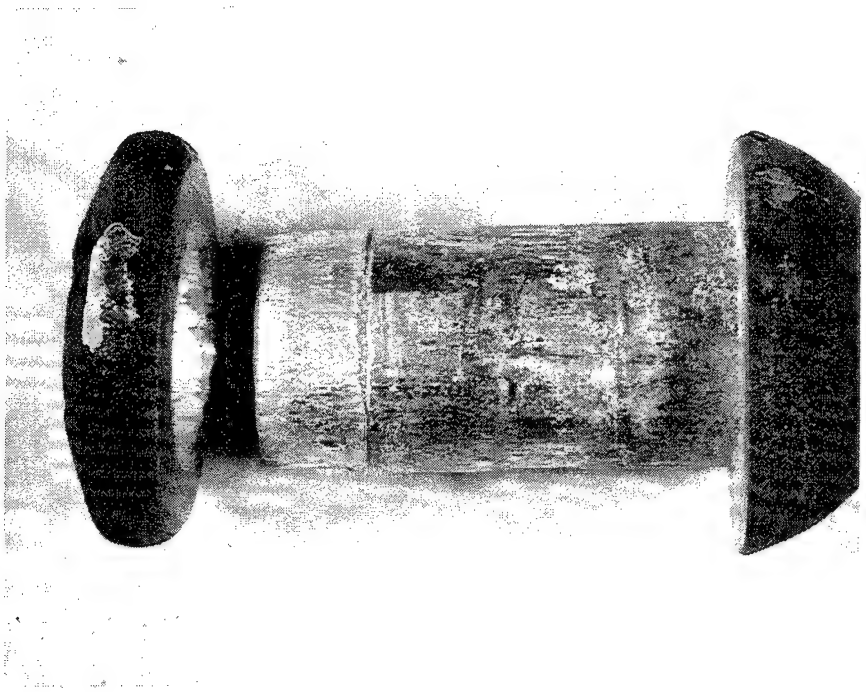

Figure 35. Enlarged view of specimen A "Good" rivet which sheared at its driven end through the rivet hole of the angle leg during the pull test. Magnification: approximately 2×.

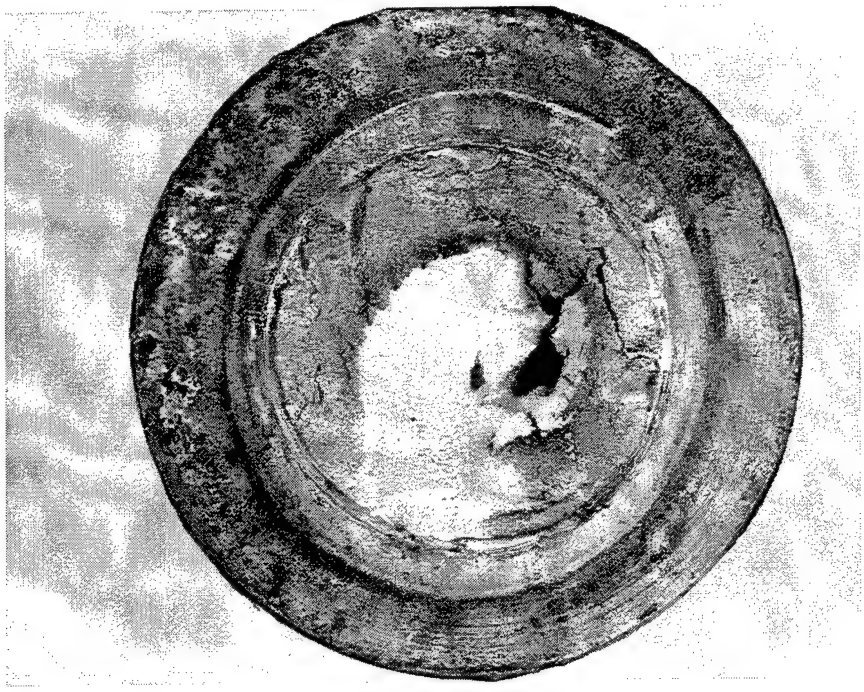

Figure 36. Enlarged view of the fracture surface under the head of specimen C "Bad" rivet after the pull test. The crack (discolored area because of corrosion) covers about 65% of the shank cross section, hence the reason for the low breaking load recorded during test. Magnification: approximately 3×.

Several cracks were observed at a higher magnification in the fillet under the head of specimen D "Bad" rivet. Therefore, the rivet head and shank section of this specimen was cut in four parts to reveal the extent of the crack because of corrosion. Figure 37 shows two quarter cross sections that revealed the cracks initiating in the fillet. One of the sections was deliberately broken apart to reveal the crack seen in Figure 38 as a discolored area on the fracture surface.

The ultrasonic inspection of the rivet specimens done in this laboratory prior to the tests did indicate a large crack in specimen C "Bad" rivet easily as revealed by the pull test when its cracked head broke off at a low breaking load. However, it did not clearly indicate a crack in specimen D "Bad" rivet. Perhaps the crack was narrow in the fillet on one side under the head. The shear strengths obtained from the double shear tests were about 43,000 psi for the "Good" rivets and 38,000 psi for the "Bad" rivets.

2.9 Clamping and Breaking Loads of New Hot-Driven AVLB Aluminum Rivets. Additional data on the clamping and breaking loads were obtained for the new aluminum alloy 7277 rivets that were hot-driven at ANAD. In this case, new 0.75-in-diameter aluminum buttonhead and flat head countersunk rivets were heated to three different temperatures (860° F, 890° F, and 1,025° F) and then hot-driven to hold three 8-in-square by 0.5-in-thick aluminum plates together. Two riveted plate sets were prepared with three button heads and three countersunk rivets per set: one rivet of each type was heated to one of three temperatures and hot-driven. One of two sets was prepared differently to evaluate a high-temperature paint, whereby six rivets were painted first, heated to high temperature and then hot-driven in the painted rivet holes of the plates. The paint coating used was evaluated as part of a repair procedure to protect aluminum rivets against similar corrosive environments encountered by AVLBS in SWA. It was not considered satisfactory because of the effect of the high temperatures on the paint coating.

Each rivet plate set was cut into six specimens, each with a rivet. A total of eight specimens were large enough for the pull tests to determine the breaking loads of the rivets. The specimens were prepared for the clamping load determinations and pull tests as described earlier in this report.

The results of the clamping load determinations and pull tests of the new AVLB aluminum rivets are given in Tables 8 and 9, respectively. On the average, the buttonhead rivets have a higher clamping load (8,170 lb) than the countersunk rivets (5,020 lb). Determination of the strain for the countersunk rivets was not as straight forward as for the buttonhead rivets because of the countersunk head configuration. This is the reason for two strain determinations and two clamping loads for each countersunk rivet, based

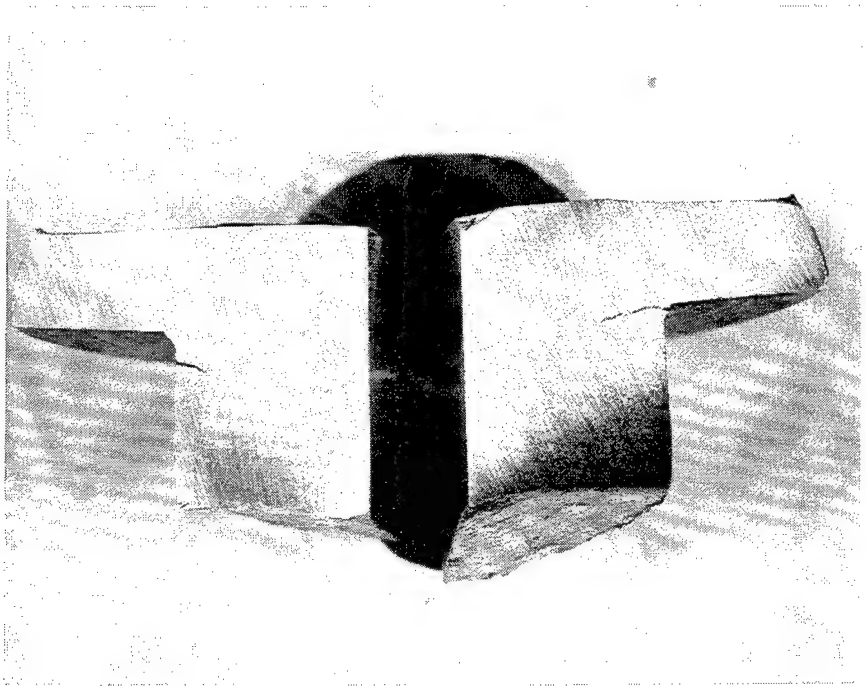

Figure 37. Enlarged view of two quarter sections of specimen D "Bad" rivet in Figure 34. Large cracks can be seen to initiate in the fillet of the right section and in the shank near the fillet of the left section. The crack on right is about 0.140-in deep. Magnification: 3×. Surface finish: Grit 600.

Figure 38. Matched cross sections of the right quarter section in Figure 37. This section was deliberately broken apart at the crack in the fillet to reveal the extent of the crack (discolored area) in the fracture surface.

Table 8. Clamping Load Determination for New Hot-Driven AVLB Aluminum Alloy Rivets

I. BUTTONHEAD RIVET SPECIMENS			
Specimen	Delta Length[a] (in)	Strain[b] (in/in)	Clamping Load (lb)
A (1,025° F-unpainted)	0.0027	0.00180	8,703
B (1,025° F-painted)	0.0030	0.00200	9,670
C (860° F-unpainted)	0.0023	0.00153	7,414
D (860° F-painted)	0.0026	0.00173	8,381
E (890° F-unpainted)	0.0026	0.00173	8,381
F (980° F-painted)	0.0020	0.0013	6,447

II. FLAT COUNTERSUNK HEAD RIVET SPECIMENS					
Specimen	Delta Length (in)	Strain (in/in)		Clamping Load (lb)	
		(A)[c]	(B)[d]	(A)	(B)
A (1,025° F-unpainted)	0.0014	0.00124	0.00107	6,017	5,158
B (1,025° F-painted)	0.0014	0.00124	0.00107	6,126	5,251
C (860° F-unpainted)	0.0007	0.00062	0.00053	3,009	2,579
D (860° F-painted)	0.0013	0.00116	0.00010	5,587	4,789
E (890° F-unpainted)	0.0017	0.00151	0.00130	7,382	6,328
F (890° F-painted)	0.0010	0.00089	0.00073	4,342	3,722

[a] Delta length of the rivet after the removal of the center plate.

[b] Total grip length to hold three 0.5-in plates together is 1.50 in.

[c] Grip length for strain calculation is based on 1.125 in.

[d] Grip length for strain calculation is based on 1.3125 in.

Table 9. Breaking Load for New Hot-Driven AVLB Aluminum Alloy Rivets (Pull Tests)

I. BUTTONHEAD RIVET SPECIMENS		
Specimen	Breaking Load (lb)	Remarks
A (1,025° F-unpainted)	30,500	Broke at fillet under head.
B (1,025° F-painted)	29,900	Broke at fillet under head.
E (890° F-unpainted)	34,000	Sheared in driven end.
F (980° F-painted)	25,900	Sheared in driven end, which was formed in an offset manner, thus lowering the breaking load.
II. FLAT COUNTERSUNK HEAD RIVET SPECIMENS		
Specimen	Breaking Load (lb)	Remarks
A (1,025° F-unpainted)	32,200	Sheared in head.
B (1,025° F-painted)	32,250	Sheared in head.
E (890° F-unpainted)	38,150	Sheared in head.
F (890° F-painted)	30,300	Sheared in head.

on two different grip lengths used. A possible reason for the apparent lower clamping loads recorded for the countersunk rivets may be due to the shrinkage of the head during cooling, which may exert less clamping force.

Specimens A and B buttonhead rivets that were heated to 1,025° F broke at the head-to-shank fillet during the pull tests, whereas specimens E and F buttonhead rivets that were heated to 890° F failed by shearing at the driven end through the rivet hole in the plate. Specimen F failed at a lower load because the driven end was formed in an offset manner, not in the center. In all cases, each countersunk rivet failed during the pull test by shearing at its head through the countersunk rivet hole in the plate (see Figure 39 for an example). The breaking loads obtained for all rivet specimens, but one was between 30,000–38,000 lb.

2.10 Pull Test on 11 AVLB Aluminum Rivet Samples From ANAD. The 11 riveted sections similar to Figure 20 were cut from the bottom or top angle chord of the AVLB from SWA and sent from ANAD

Figure 39. An example of the shearing at the flat countersunk head of unpainted 1,025° F rivet sample.

to Belvoir for the pull tests. They were labeled as "Good" (four), "Moderate" (two), or "Bad" (five) based on the ultrasonic inspection done at ANAD. They are listed in Table 10. Each sample was cut to a 3-in-wide section with the angle horizontal legs cut off. The samples were prepared and tested in the same manner as described earlier in this report so that the rivet was loaded in tension to failure.

The results of the pull tests on the AVLB rivet samples from ANAD are given in Table 11. "Good" rivet sample no. 17 broke at a lower load (27,000 lb) at the head-to-shank fillet because it contained a small crack under the head as the result of corrosion. The condition of this sample was questionable initially during the ultrasonic inspection at ANAD, because "Good?" was written on it. Nevertheless, it was labeled "Good" and submitted for the pull test. The other "Good" rivet samples failed at loads above 30,000 lb in the pull tests when they sheared at their driven end through the rivet hole in the angle vertical leg. The size of the driven end formed during the rivet installation can have an important effect on where the rivet failed during the pull tests. Based on this and previous tests, the driven ends that were formed with the shallow configuration invariably sheared through the rivet hole in the part, whereas the driven ends formed with thick configuration did not shear, but the rivets broke either at the fillet or in the shank.

Table 10. Description of AVLB Aluminum Rivet Samples from ANAD

Sample No.	Status	Angle Chord	Rivet Hole	
			Position	Remarks
16	Good	Bottom	High	—
17	Good	Top	High	"Good?" was also written on this sample.
20	Good	Top	Low	—
21	Good	Top	Low	"Good?" was also written on this sample.
7	Moderate	Bottom	High	—
14	Moderate	Bottom	High	—
4	Bad	Bottom	Low	—
6	Bad	Bottom	High	—
8	Bad	Bottom	High	—
9	Bad	Bottom	High	—
18	Bad	Top	Low	"Good?" was written on this sample, but it was crossed out.

Depending on the extent of prior cracks from corrosion (stress corrosion cracking), all "Moderate" and "Bad" rivet samples broke at the fillet under the head during the pull tests, with the breaking loads ranging from 5,500 to 26,550 lb. "Bad" rivet samples nos. 4 and 9 broke at much lower loads because of large cracks as compared to those in other rivet samples that broke at higher loads. Figures 40 and 41 show the enlarged views of the fracture surfaces, revealing the sizes of the cracks from corrosion in eight samples that broke at the fillet under the head. The estimated percentages of the corroded cracks observed in the fractures of the rivets ranged from 8 to 95.

Extensive white corrosion products were observed on the surfaces of the aluminum parts (rivet, plate and angles) in contact with each other in "Good" rivet sample no. 17 and all "Moderate" and "Bad" samples, more so than the other "Good" samples. After the pull tests, the three "Good" rivets that sheared at their driven end during the tests were examined visually at a higher magnification for the cracks in the fillet under the head. No visible cracks were observed in the fillet of those rivets, verifying the findings of the ultrasonic inspection as being "Good."

Table 11. Pull Tests on AVLB Rivet Samples

Sample No.	Breaking Load (lb)	Remarks
16 (Good)	33,400	Sheared at driven end, shear strength of about 41,050 psi.
17 (Good)	27,000	Broke at head-to-shoulder fillet, has about 8.45% prior crack from corrosion, tensile strength of 57,230 psi.
20 (Good)	31,700	Sheared at driven end, shear strength of about 41,320 psi.
21 (Good)	33,000	Sheared at driven end, shear strength of about 40,920 psi.

Sample No.	Breaking Load (lb)	Tensile Strength (psi)	Percent Prior Crack (%)
7 (Moderate)	26,550	56,280	11.39
14 (Moderate)	25,450	53,950	26.95
4 (Bad)	5,500	11,660	95.37
6 (Bad)	25,400	53,840	19.62
8 (Bad)	24,850	52,680	11.60
9 (Bad)	13,850	29,360	67.75
18 (Bad)	23,450	49,710	17.73

NOTES:

"Good" no. 17, all "Moderate" and all "Bad" rivet samples broke at head-to-shoulder fillet.

Shear strength was determined approximately by measuring the sheared area at the driven end of the rivet sample that had sheared through the rivet hole during the pull test.

2.11 Push Tests on Corroded AVLB Aluminum Rivets Without the Manufactured Heads. A number of aluminum alloy 7277 buttonhead rivets on the AVLB that was brought back to the U.S. from SWA after the Operation Desert Storm War and stored at ANAD were found with their manufactured heads already fallen off (see Figures 2 and 3) because of the corrosion. Some of those rivets can be driven out of the rivet holes with the hammer and a drift pin. Other rivets cannot or were hard to be driven out because of the extensive white corrosion products formed on the rivet shanks and rivet holes. Two types (plunger and dowel pins) of the push tests were performed on the headless corroded AVLB rivets in order to determine the amounts of the load required to drive them out of the rivet holes.

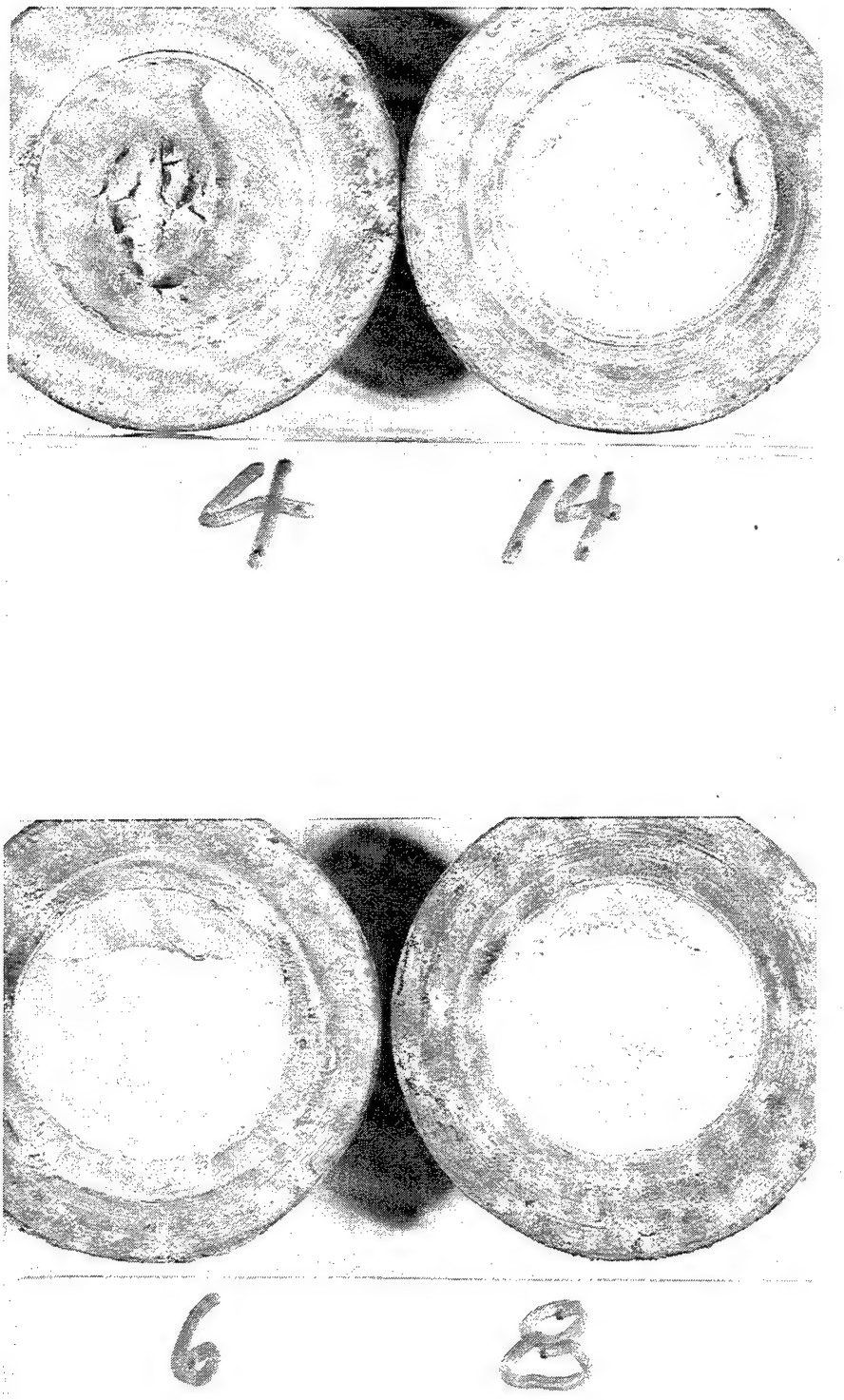

Figure 40. Enlarged views of the fracture surface under the buttonhead of four rivet samples after the pull tests revealing the extent of cracks (darkened area) observed due to corrosion. Sample 4 (95.37%), no. 14 (26.95%), no. 6 (19.62%), and no. 8 (11.60%).

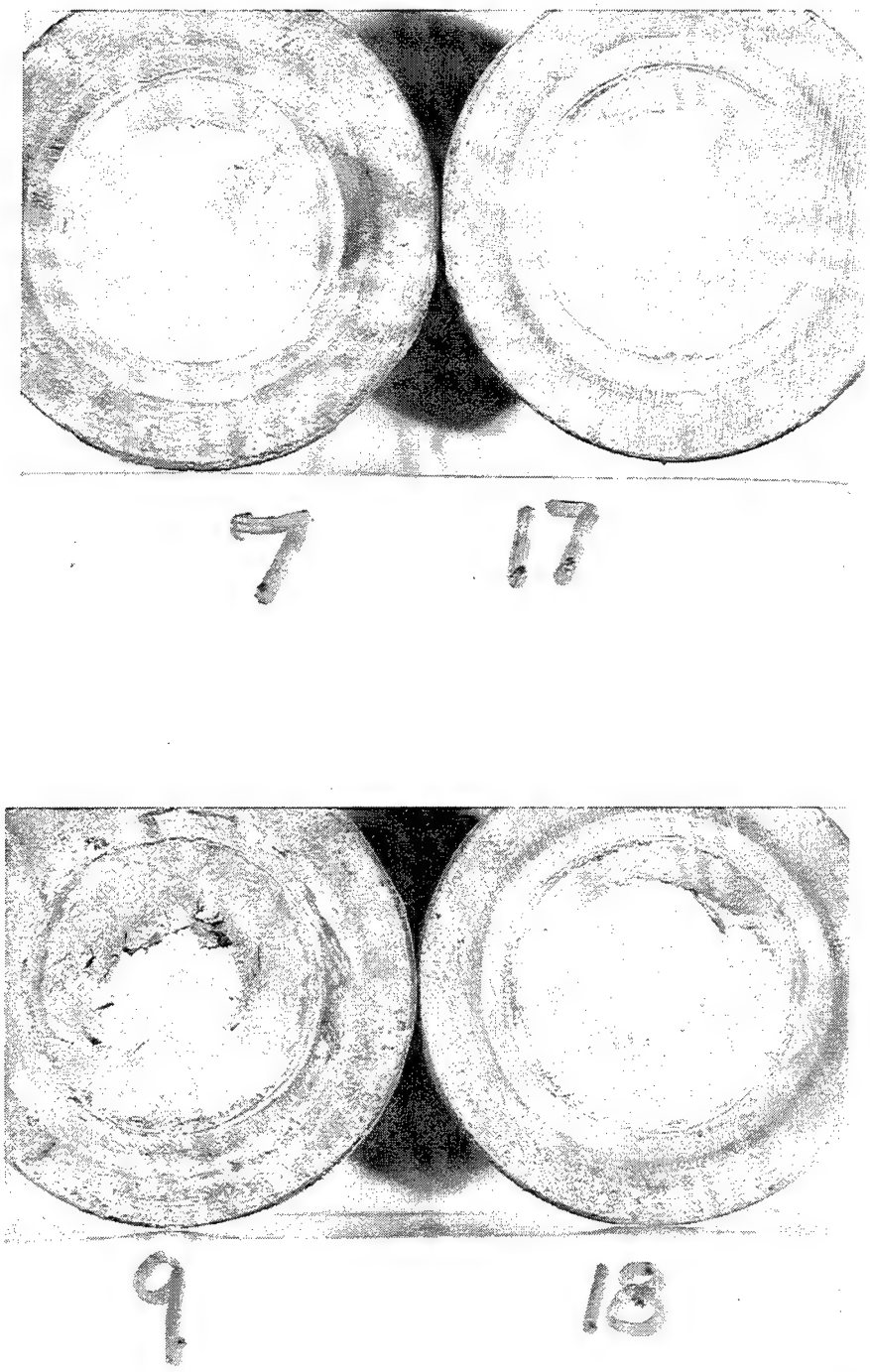

Figure 41. Enlarged views of the fracture surface under the buttonhead of four rivet samples after the pull tests, revealing the extent of the cracks (darkened areas) observed. Sample no. 7 (11.39%), no. 17 (8.45%), no. 9 (67.76%), and no. 18 (17.73%).

Although the corroded rivets with their manufactured heads already fallen off were not available or not found for the push tests, four small sections similar to Figure 20 were cut from AVLB riveted aluminum angle chords (top or bottom) at ANAD and sent to Belvoir for the tests. The rivet heads remained intact, although the ultrasonic inspection done at ANAD indicated that they contained defects, such as cracks. The submitted sections containing the rivets were labeled as "5," "10," "12," and "15." Three of them were marked as "Bad" and the fourth as "Good?," based on the results of the ultrasonic inspection at ANAD. Initially, the manufactured rivet heads could not be knocked off without severe hammering for fear of affecting the integrity of the corroded rivets in the rivet holes. Finally, the head was cut off from each rivet sample with the band saw, and the cut end of the shank was ground flush to the surface of the assembled section, removing the remaining portion of the head.

Two types of the push tests were performed on the headless rivets still in the assembled sections. For the plunger tests, a plunger with its diameter slightly smaller than the rivet hole, was used on the headless end of the rivet to push it through the rivet holes, emerging from the driven end side of the section. Two headless rivet samples were tested by this method. The other push test used the steel pins to push the two outer angle legs apart from the center girder plate. This test method was similar to the pull tests done previously on the rivets with their head. Three 0.5-in-diameter holes 120° apart around the rivet were drilled on both sides of the assembled section (see the sketch mentioned earlier) so that the angle legs will be pushed apart by the dowel pins in the drilled holes when loaded in compression. The other two headless rivet samples were tested by this method. After the tests, small sections were cut from the headless end of two rivet samples as metallographic specimens. They were mounted, ground, polished, and etched for microstructural examination for cracks as the results of the corrosion.

The results of the push tests on four headless rivet samples in the assembled sections are given in Table 12. Rivet sample 10 required the highest load (9,880 lb) in order to be pushed out of the rivet holes in the angle legs and girder plate of the assembled section. Other three headless samples required much lower loads (200–300 lb) to be pushed out. The main difference was in the amount of white corrosion products observed on the shank of each rivet sample as well as in the rivet holes. The corrosion products increased in volume when formed on the corroded aluminum surface, causing the rivet to bind in the holes to the point that it couldn't be driven out, at least not easily. This was the reason why some corroded rivets with their heads already fallen off could not be or were hard to be driven out of the holes because of extensive corrosion products formed.

Table 12. Push Tests of Corroded AVLB Rivets Without Their Manufactured Heads

I. PLUNGER PUSH TEST WITH A PLUNGER		
Sample	Maximum Load (lb)	Remarks
15 (Good?)	260	Rivet shank and holes were slightly pitted.
10 (Bad)	9,880	Thick, white corrosion products on the rivet shank and inside the rivet holes.
II. DOWEL PINS PUSH TEST		
12 (Bad)	300	Rivet shank and holes were slightly pitted.
5 (Bad)	200	Rivet shank and holes were slightly pitted.

NOTE: Since the manufactured heads of the corroded AVLB rivet samples could not be knocked off with the hammer and chisel easily, they were cut off with the band saw before the push tests. The cut ends of the rivet shanks were ground flush to the surface of the assembled section by grinding.

As seen in Figure 42, the driven end of rivet sample 10 was much larger in size as compared to sample 15. Also, it was formed off center. Apparently, a longer length rivet instead of the correct length was used in this case, resulting in the large size driven end in off-centered position. Because of this situation, water or moisture probably entered at the point where the driven end flange was very narrow, which led to extensive formation of the white corrosion products on the shank of sample 10 as well as in the rivet holes of the assembled section. After the tests, significant amounts of the corrosion products were observed on the surfaces of the angles and girder plate in contact with each other, indicating that corrosion had occurred on the AVLB.

In addition, visual examination of the headless ends of the rivet samples after the tests, revealed cracks in the cut end and in the fillet, which verified the indications of cracks by the ultrasonic inspection prior to the tests. Figure 43 shows the etched cross sections of two headless corroded samples 10 and 15, after the push tests, revealing stress corrosion cracks at the fillets. Figures 44–47 are the as-polished and etched microstructures in the cut end of samples 10 and 15. Those cracks were near the fillet. They followed the grain flow produced by the forming of the rivet head by the rivet vendor. The findings were the same found on the corroded AVLB rivets investigated previously, confirming that the primary cause of the rivet failure was due to stress corrosion cracking.

Figure 42. A view of the headless AVLB aluminum rivet samples 10 (left) and 15 after the plunger push tests, revealing the condition of the corroded rivet shanks. A load of 9,880 lb was required to push sample 10 out of the rivet holes as compared to 260 lb for sample 15. Note the complete coverage of thick white corrosion products on the shank surface of sample 10 vs. small corrosion pittings on sample 15. Also, note the larger size, off-center driven end of sample 10 as compared to the normal, centered end 15. This was due to use of incorrect, longer length rivet (sample 10), which probably allowed moisture to enter into the rivet hole at the very narrow flange (left side of sample 10) of the driven end, resulting in extensive formation of corrosion on the rivet shank surface. Magnification: 1.33×.

In order to determine the load required to push a noncorroded rivet out of the rivet holes, additional plunger tests were performed on the new rivets on the thick assembled aluminum plate sample consisting of a 0.5-in plate between two 1-in-thick plates. Two new rivets, one was heated to 860° F and the other to 890° F, were hot-driven in the rivet holes of the thick plates to form a 2.5-in-thick assembled block, which was done at ANAD and sent to Belvoir for the tests. The rivets were subject to the plunger tests after their heads were cut off to simulate the headless rivets. The 860° F rivet required 500 lb and the 890° F rivet 900 lb to be pushed out of the rivet holes of the 2.5-in-thick assembled block. It should be noted that rivet sample 15 with little corrosion required 260 lb to be pushed out of the holes through three 0.375-in-thick angle legs and girder plate for a total of 1.125 in thick.

Depending on the amounts of the white corrosion products formed on the rivet shanks and in the rivet holes, the corroded AVLB rivets with their manufactured head fallen off stayed in the rivet holes. When no tension load is involved and the riveted parts remain together, the headless corroded rivets remaining in the holes can still function properly as long as the loads acting on them are in shear, not in tension, until the repairs can be made on the bridge when appropriate.

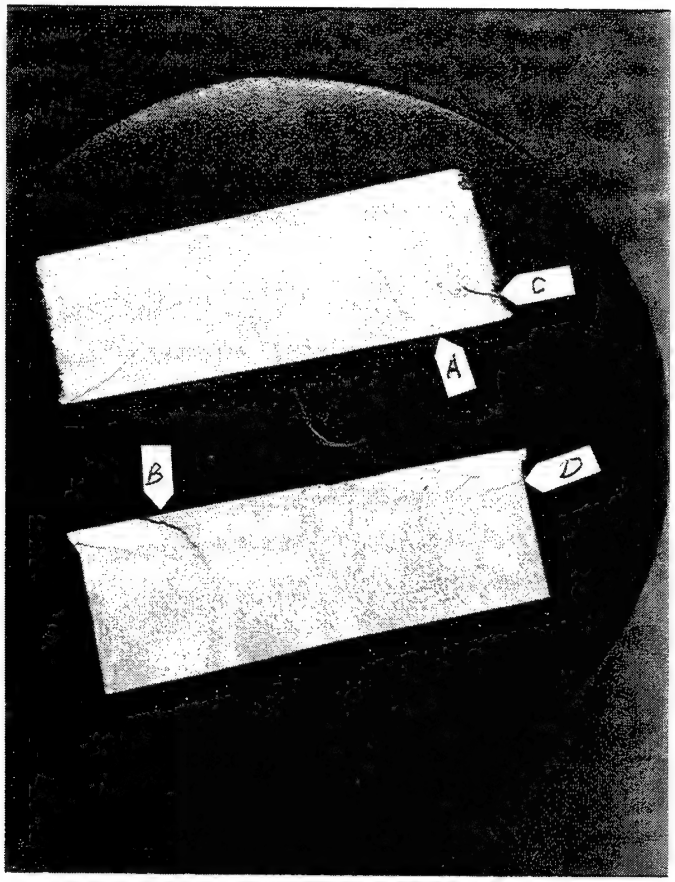

Figure 43. Enlarged view of the etched cross sections of the corroded AVLB rivet samples 10 (top) and 15, revealing stress corrosion cracks (dark curved lines) in the headless ends (arrows A and B) where the rivet buttonheads were sawed off. Most cracks observed were initiated at or near the fillets (partly seen in the photograph) and followed the grain flow caused by the head-forming operation. The microstructure at arrow C is seen in Figures 44 and 45, and that at arrow D in Figures 46 and 47. Magnification: 3.17×. Keller's etchant.

2.12 Initial Visual Inspection of a Corroded AVLB (MLC-60 Tons). A corroded AVLB (MLC-60 tons) was inspected at Fort Stewart, GA, by ANAD personnel using an ultrasonic inspection method to locate corroded aluminum rivets with cracks in their manufactured heads. After the inspection, the bridge was disassembled and shipped to Fort Belvoir for the fatigue tests to determine what the effects of cyclic fatigue loadings would have on the corroded rivets, particularly on those without their heads.

The corroded AVLB shipped to Belvoir was reassembled together in the bridge hangar to be placed under the load frame for the fatigue tests. It has the desert sand color and markings to indicate it was in SWA. Furthermore, it had been used in the field practices at Fort Stewart. There were eight corroded rivets, mainly in the forged aluminum connectors, which already had their heads deliberately knocked off

Figure 44. As-polished microstructure of stress corrosion cracks on the shank of corroded rivet sample 10 near the fillet. Note the integranular corrosion on the surface of the shank (right side) and in the major cracks. Magnification: 100×.

based on the results of the ultrasonic inspection. The paint coating had flaked off or peeled loose in a number of places on the AVLB, exposing the aluminum metal to the corrosive environments. White corrosion products had already formed on the exposed aluminum metal and under the loose paint, even on the rivet heads, and were observed on the fracture surface of the rivets with heads deliberately knocked off, indicating cracks as the result of stress corrosion cracking. A number of rivets were already marked as having cracks as indicated by the ultrasonic inspection done at Fort Stewart.

The initial visual inspection of the AVLB (fabricated under Contract DAAE07-86-C-2797) was performed prior to the fatigue tests, which will be conducted by the Bridge Division of the Mobility Technology Center-Belvoir. Ten visible cracks were found on the bridge. Seven of them were located in the vertical aluminum structural angles of the cross members inside the end panel assemblies. In each case, a longitudinal crack, as long as 3 in, had occurred through the bottom rivet hole of the angle leg riveted to the inboard girder plate. No visible cracks were observed in the critical areas such as the

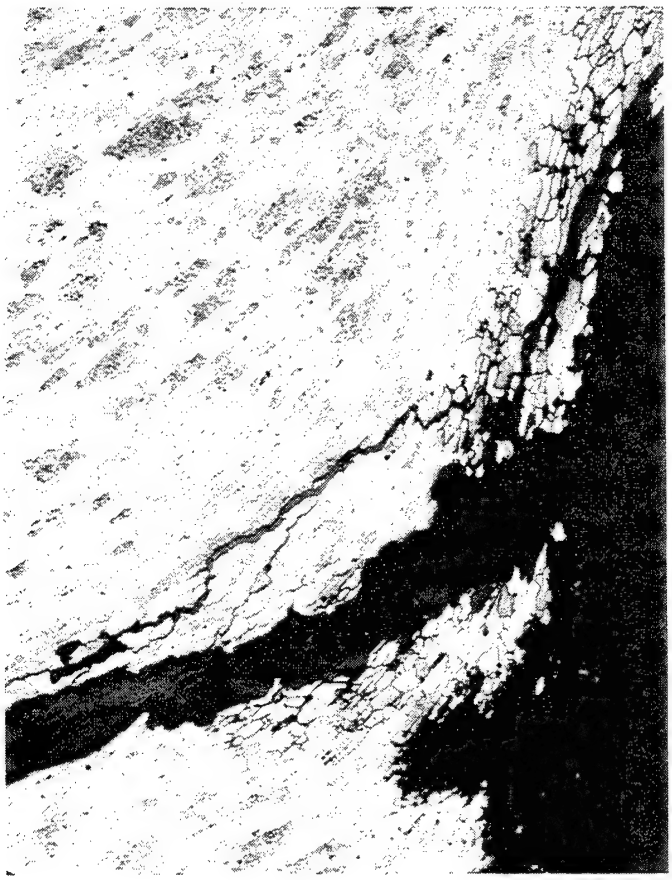

Figure 45. Etched microstructure of the same area in Figure 44, showing the grain flow formed by the head-forming operation. Magnification: 100×. Keller's etchant.

forged aluminum center hinges, the bottom forged aluminum connectors, and the aluminum plate splices that joined the steel ramp end section to the aluminum section of the end panel assemblies. The crack location/type found were typical of several other AVLBs previously inspected at Belvoir.

Meanwhile, ANAD personnel came to Belvoir, reinspected the aluminum rivets, and recorded the ultrasonic data into the computer to establish the baselines prior to the fatigue tests. They would come back to Belvoir from time to time to reinspect the same rivets after the AVLB had undergone specific number of cyclic loadings under different loading conditions. This was to determine if there had been changes to the initial ultrasonic data to indicate propagation of the cracks in the corroded rivet heads as indicated by the ultrasonic readings made prior to the fatigue tests. Also, marks were made on eight headless rivets to indicate their rotation, if any, in the rivet holes during the cyclic loadings of the AVLB.

Prior to the deliberate overload of the AVLB to failure after completion of all the planned fatigue tests, no changes were noted on the initial ultrasonic data of the rivet inspection, indicating no apparent cracks propagation. No rivet heads had popped or fallen off, and none of the eight headless rivets had rotated or even moved in their rivet holes.

Figure 46. As-polished microstructure of stress corrosion cracks on the shank of the corroded sample 15 near the fillet area. Note the integranular corrosion (not clearly seen in this photograph) on the surface of the shank (left side) and in the major crack. Magnification: 100×.

2.13 Push-Out Tests of Aluminum Rivets From Corroded AVLB. A special load jig was fabricated and used to push out a number of headless 0.75-in-diameter aluminum from a corroded AVLB after it had undergone a series of fatigue tests to simulate 3,000 crossing load cycles under the load frame in the Belvoir Center Bridge Hangar. After the final deliberate overloading of the bridge to failure, a broken female center panel assembly (S/N 285, NSN 5420-00-542-3115, Contract DAAE07-86-C-2797) was removed from the failed bridge and set aside for the rivet push out tests. It contained several headless corroded rivets mentioned previously during the initial visual inspection of the corroded bridge.

The special load jig (see Figure 48) for the tests was designed and fabricated so that it can be clamped to the horizontal legs of the aluminum chord angles and forged connectors on the bottom or top chord of the AVLB center or end panel assembly. It had a hydraulic cylinder with a hand pump and load dial. The jig was clamped to the bridge top chord and connector by bolts and plates in line with the headless rivet to be pushed out (see Figure 49). A 0.5-in-diameter steel bar 2 in long with two strain gauges on

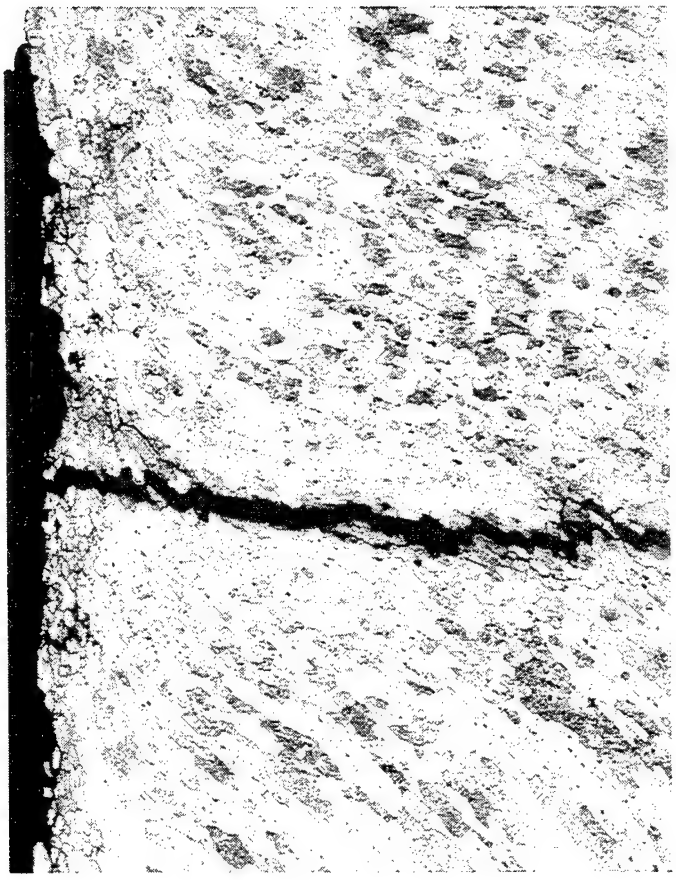

Figure 47. Etched microstructure of the same area in Figure 46, showing the grain flow formed by the head-forming operation. Magnification: 100×. Keller's etchant.

opposite sides was placed between the headless end of the rivet and the plunger of the hydraulic cylinder (see Figure 50). The strain gauges on the pin indicated the loads applied to the rivet being pushed out. The pin was calibrated so that the strain readouts on the strain indicator can be read as pounds instead of microinches. Another steel pin with two strain gauges was used as the compensating component ("dummy") in the strain indicator instrumentation setup. The maximum load required to break the rivet loose in its holes was recorded during the test.

Seven aluminum rivets were tested during the push out tests: three headless corroded rivets and four rivets with their heads removed by grinding. The description of the rivets tested and the test results are given in Table 13. The no. 1 corroded headless rivet broke loose in the rivet holes after a load of 19,000 lb was applied to it. Its shank was covered with thick white corrosion products which were also observed in the rivet holes of the chord angles, connectors, and girder plate. Because of the volume buildup of the corrosion products, the rivet was bound in its hole, requiring considerable load to break it

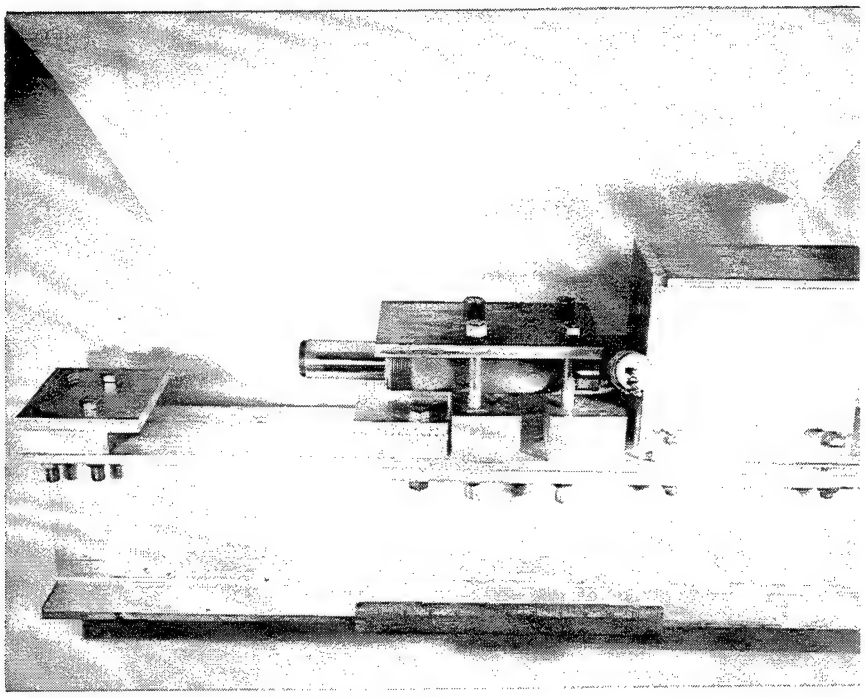

Figure 48. A view of the special push load jig after the fabrication. A small hydraulic cylinder is clamped to the aluminum I-beam with aluminum plate and blocks and steel bolts. It is butted against the upper I-beam, serving as a backstop.

loose. The no. 2, 3, and 6 rivets did not break loose in their rivet holes, even at loads up to 20,000 lb, which was the maximum load that can be applied by the special jig, and the test was terminated. The three rivets (nos. 4, 5, and 7) with their head ground off broke loose at loads between 500 and 1,500 lb. Little corrosion products had occurred on the surface of their shank, leading to the reason for low loads required to break them loose in the rivet holes. The difference in the buildup of the corrosion products on the shank of several rivets is seen in Figure 51.

Based on the limited number of push-out tests performed in this work on the AVLB corroded rivets, they, without their heads, required considerable force to break loose in the rivet holes. The heavy buildup of the white corrosion products between the rivet shank and the rivet holes played an important role in binding the corroded rivet in the rivet holes. Those rivets did not become loose as the result of the fatigue tests of 3,000 simulated crossings performed on the corroded AVLB and after the final failure of the bridge by overloading.

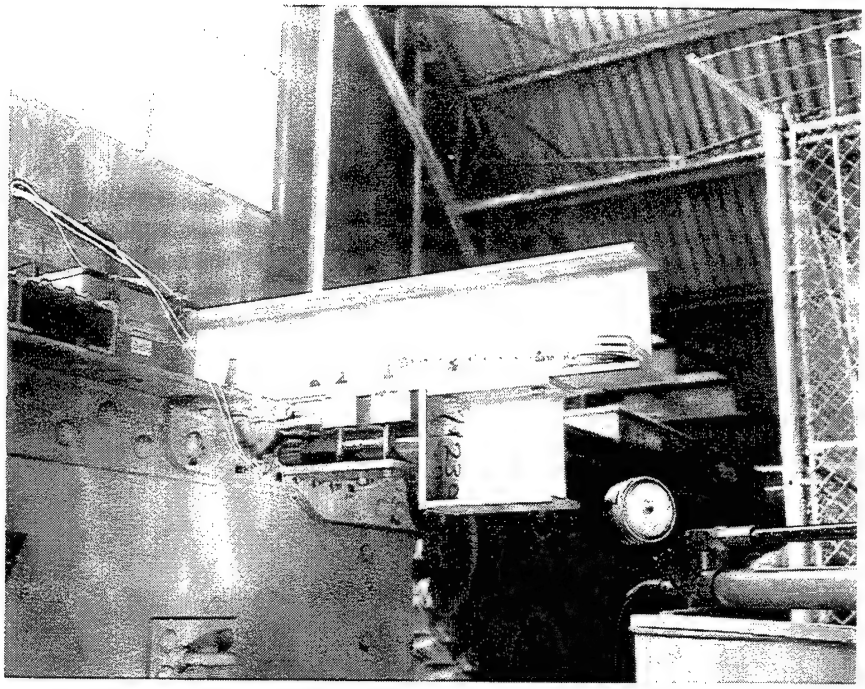

Figure 49. Overall view of the special load jig clamped to the top outboard male connector of the AVLB female center panel assembly by means of bolts and plates. The hydraulic cylinder and its hand pump are seen in this photograph. Three extruded aluminum deck panels had to be removed from the top of panel assembly in order to perform the test.

2.14 Metallurgical Examination of the Fractures of Several Failed Major Aluminum Components of Corroded AVL Bridge After the Overload Test. After a series of fatigue tests to simulate 3,000 crossings was performed on the corroded AVLB (from Fort Stewart) under the load frame at the Belvoir Center Bridge Hangar, a visual inspection of this bridge for new cracks was performed before the static overload test to failure. A major crack was found on the inner aluminum angle of the inboard bottom chord at the first rivet hole in the forged aluminum center hinge of two male center panel assemblies S/N 176 and S/N 178 (Contract DAAE07-86-C-2797). It was speculated that a catastrophic failure of the bridge may occur at one of those two cracks in the bottom chord angles during the overload test. A series of major component failures occurred on the bridge as the static loads increased during the test, but the final catastrophic failures did not occur in either crack located in the cracked bottom chord angles.

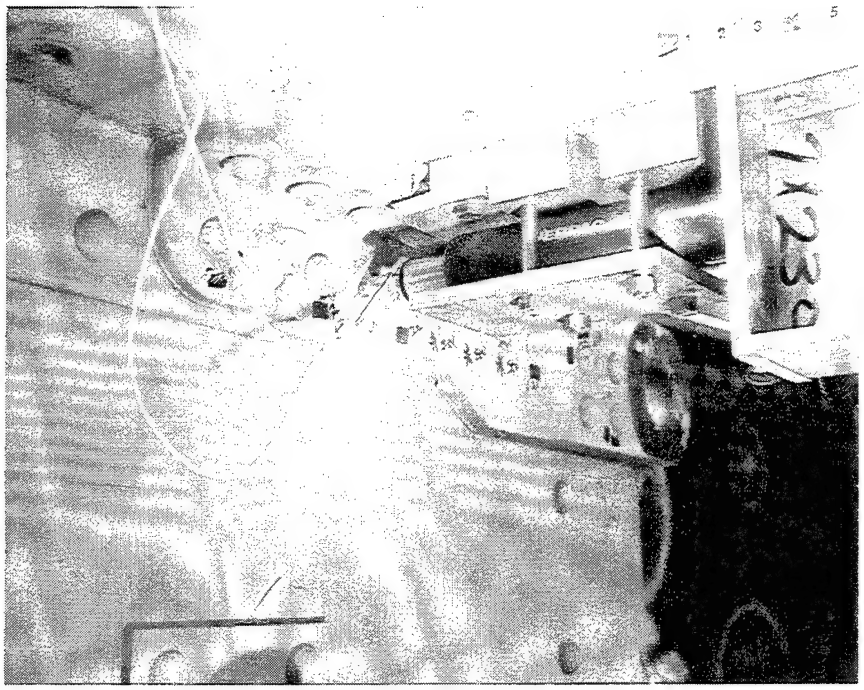

Figure 50. Closeup view of the special jig in Figure 49, showing the placement of the 0.5-in-diameter steel pin (with two strain gauges) between the headless end of the rivet and the plunger end of the hydraulic cylinder. This jig was setup for the testing of the no. 4 rivet. The cables from the strain gauges were connected to the strain indicator not seen in this photograph.

The sequence of major component failures during the overload test occurred as followed:

(1) At 95 tons, a loud popping noise was heard, and the test was stopped. The load was released in order to determine the cause of the noise. The eye of the outer forged aluminum female center hinge, on the inboard side of the female center panel assembly S/N 285, was found broken through the 3-in-diameter hole. The broken piece is seen in Figure 52.

(2) At higher loads, more popping noises were heard, but the sources of the noises could not be found after the test was stopped again.

(3) At 115 tons, the bridge broke catastrophically. Inspection of the bridge after the test revealed that the major failures occurred in the inboard and outboard bottom chord male forged aluminum connectors of the female center panel assembly S/N 214 and in the other forged female center hinge eye of the same center panel mentioned in paragraph (1) of this section. The eyes of the

Table 13. Description of the Aluminum Rivets Tested and Results of the Push-Out Tests

No.	TOP OUTBOARD MALE CONNECTOR
1	Corroded rivet with no head (next to A21 rivet). Required a load of 19,000 lb to break loose in rivet holes. Its shank and the rivet holes were covered with thick white corrosion products.
2	Corroded rivet with no head (next to No. 1 rivet). It did not break loose after a load of 20,000 lb was applied. This would indicate volume buildup of the corrosion products to bind it in the rivet holes.
3	Corroded rivet with no head (next to A22 rivet). Same comments as no. 2 rivet.
4	Rivet with its head ground off (between A22 and A23 rivets). It broke loose after a load of 1,200 lb was applied. Little corrosion products had occurred on the surface of its shank.
5	Rivet with its head ground off (between A23 and A24 rivets). It broke loose after a load of 1,500 lb was applied. Little corrosion products had occurred on the surface of its shank.
6	This rivet was labeled as A24 for ultrasonic inspection purposes by ANAD personnel. Its head was ground off. However, cracks and heavy corrosion products were observed in the head during the grinding operation. The rivet did not break loose after a load of 20,000 lb was applied, indicative of heavy corrosion product volume buildup to bind it in the rivet hold, as happened with no. 2 and 3 rivets.
	TOP INBOARD MALE CONNECTOR
7	Rivet with its head ground off (between J19 and J20 rivets). It broke loose after a load of 500 lb was applied. It contained less corrosion products on the surface of its shank than the no. 4 and 5 rivets.

NOTES: No. 4, 5, and 7 rivets were not labeled for the ultrasonic inspection purposes.

outboard male connector broke at the sharp fillets machined on the sides of the connector forgings (see Figure 53). The eyes of the inboard male connector broke in half through the hole seen in Figure 54. Visual examination was made on the fractured surfaces of the major failed components. Figures 55 and 56 reveal that the initiation sites of the brittle fractures of the outer female center hinge had occurred at a small fatigue crack at the surface of the eyehole. Figures 57 and 58 reveal the small fatigue cracks initiated at the sharp machined fillets that led to the brittle failure of the outboard male connector eyes. Figure 59 shows small fatigue cracks at the surface of the eyehole of the inboard male connector. The samples containing the crack in the bottom chord angles found during the visual inspection before the overload test were cut out in order to view the fractured surfaces (see Figure 60). Again, small fatigue cracks were observed initiating at the bottom of the countersunk rivet hole of one sample (see Figure 61). Figure 62 shows the extent of corrosion on the underlying surfaces next to the aluminum connector forging.

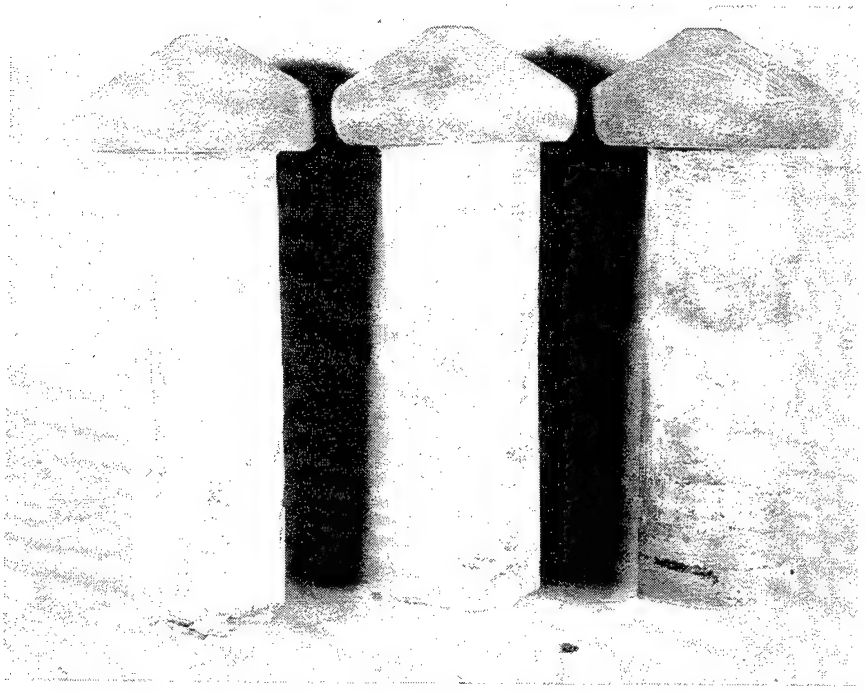

Figure 51. A view of the white corrosion products on the surface of the shank of the no. 1 headless corroded rivet at left, no. 5 rivet in middle, and no. 7 rivet at right. The loads required to break the rivets loose in their rivet holes were 19,000 lb for no. 1; 1,500 lb for no. 5; and 500 lb for no. 7.

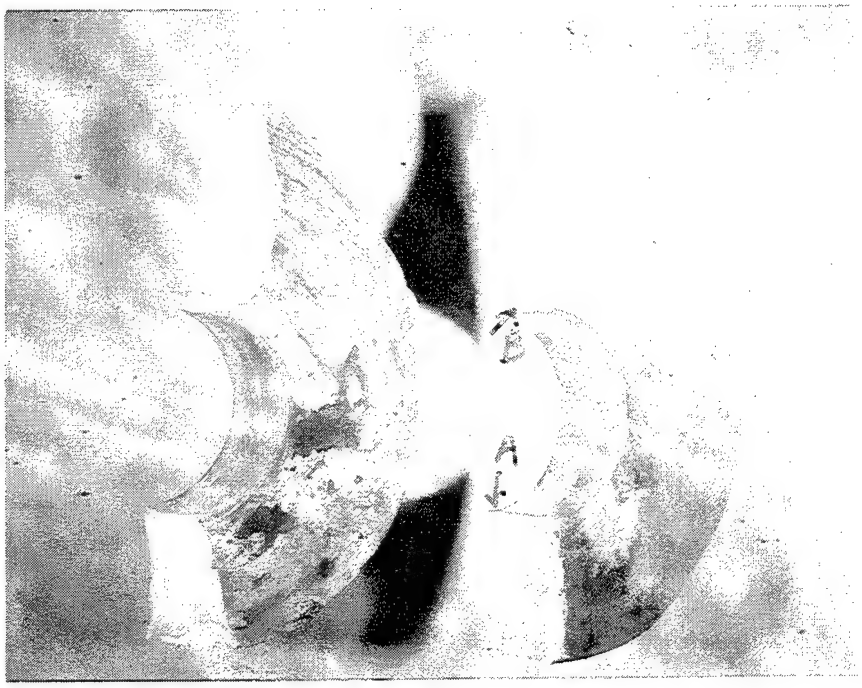

Figure 52. View of broken inboard female center hinge eyes. The piece on left is part of the inner hinge forging, and the other piece is part of the outer hinge forging that broke first at 95-ton load. Small fatigue cracks at A and B are seen in Figures 55 and 56.

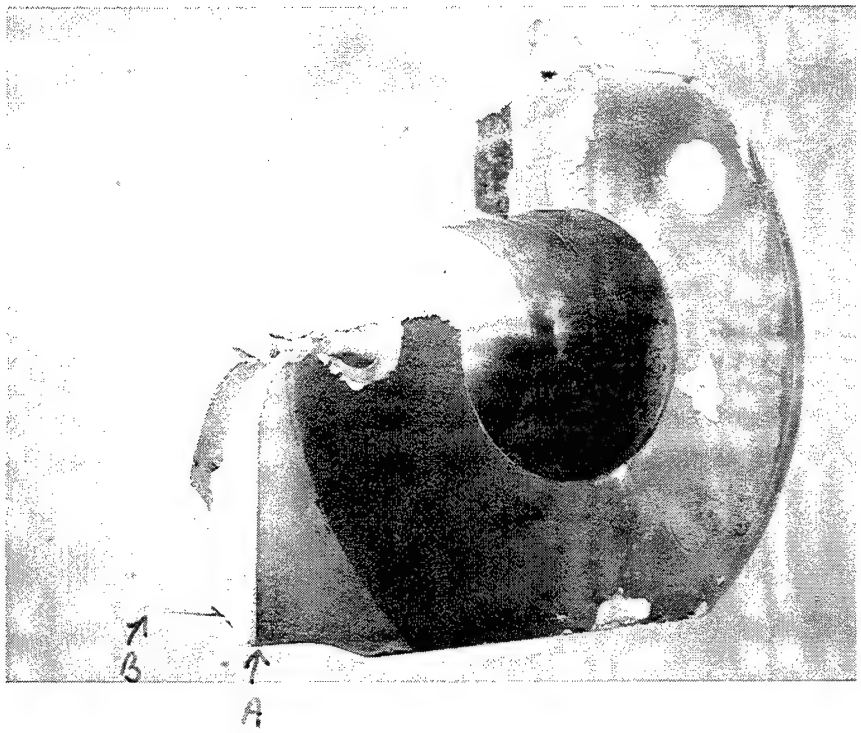

Figure 53. View of broken outboard bottom chord male connector eyes from the female center panel assembly after the failure test. The brittle fractures initiated at A and B because of the sharp machined fillets (straight edges). Closeup views of small fatigue cracks at A and B are seen in Figures 57 and 58.

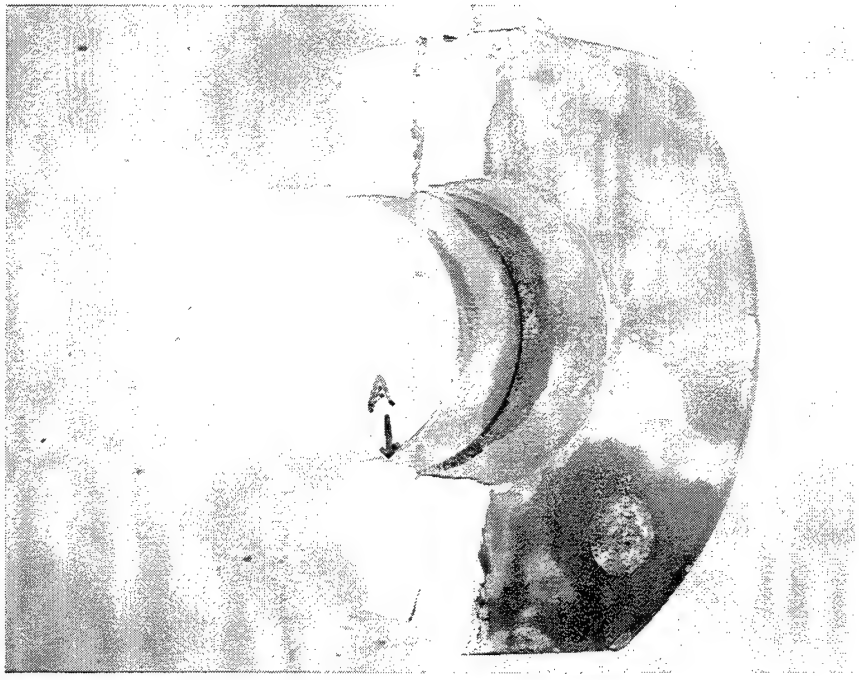

Figure 54. View of broken inboard bottom chord male connector eyes from the female center panel assembly. See Figure 59 for closeup view of the crack initiation site at A.

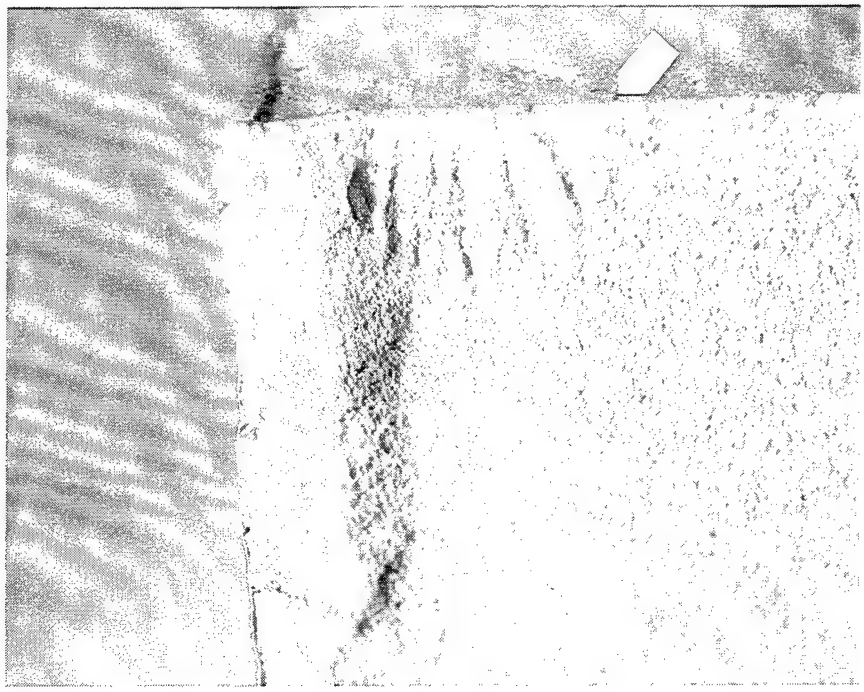

Figure 55. Closeup view of a small fatigue crack (arrow) at A in Figure 52. This eye piece of the forged female center hinge broke first at 95-ton load, initiating at this fatigue crack.

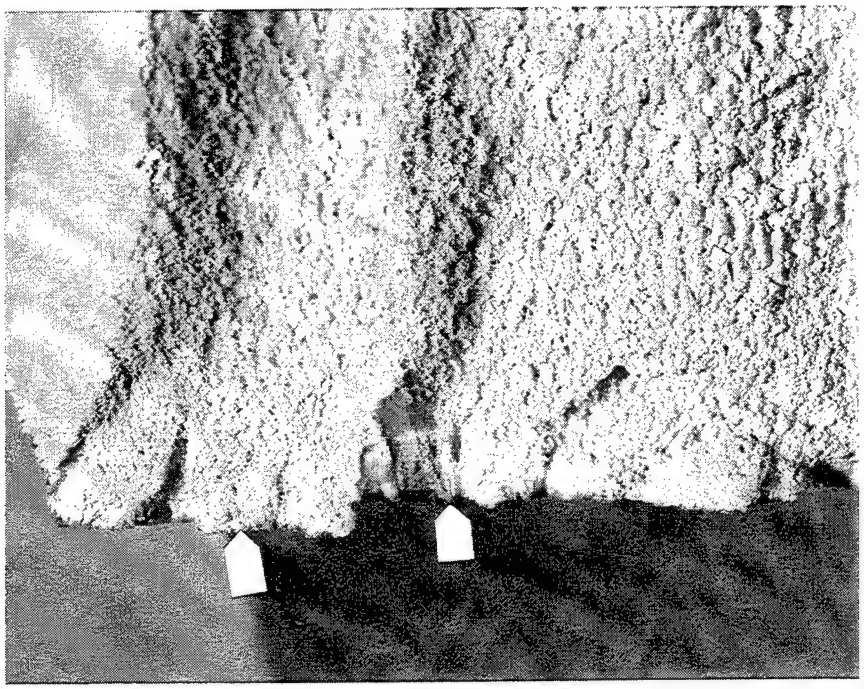

Figure 56. Closeup view of small fatigue crack (top edge) at B in Figure 52 after the eye piece broke from the forged female center hinge at 115-ton load.

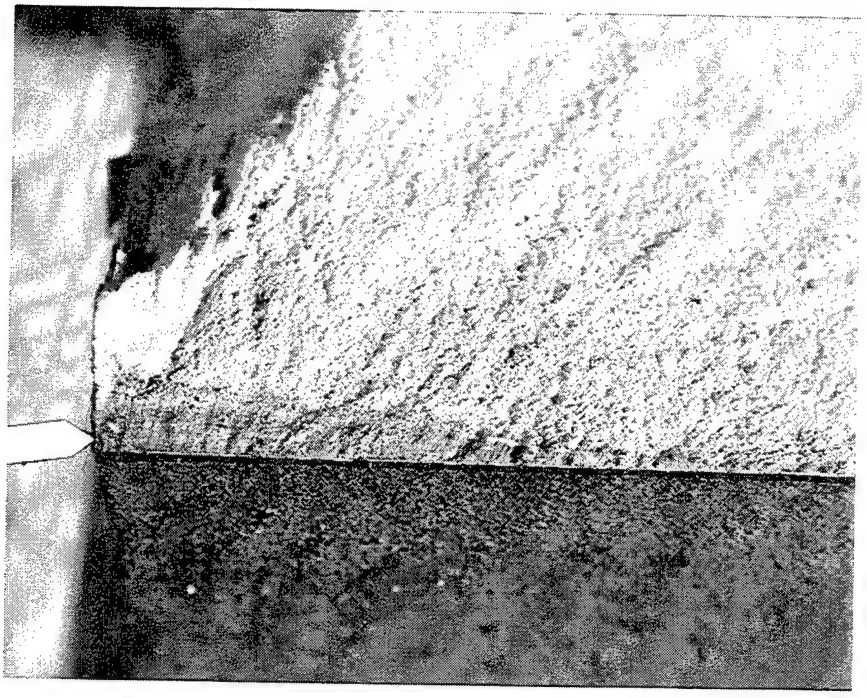

Figure 57. Closeup view of a small fatigue crack (arrow) at A in Figure 53 where it was initiated at the sharp machined fillets (straight edge).

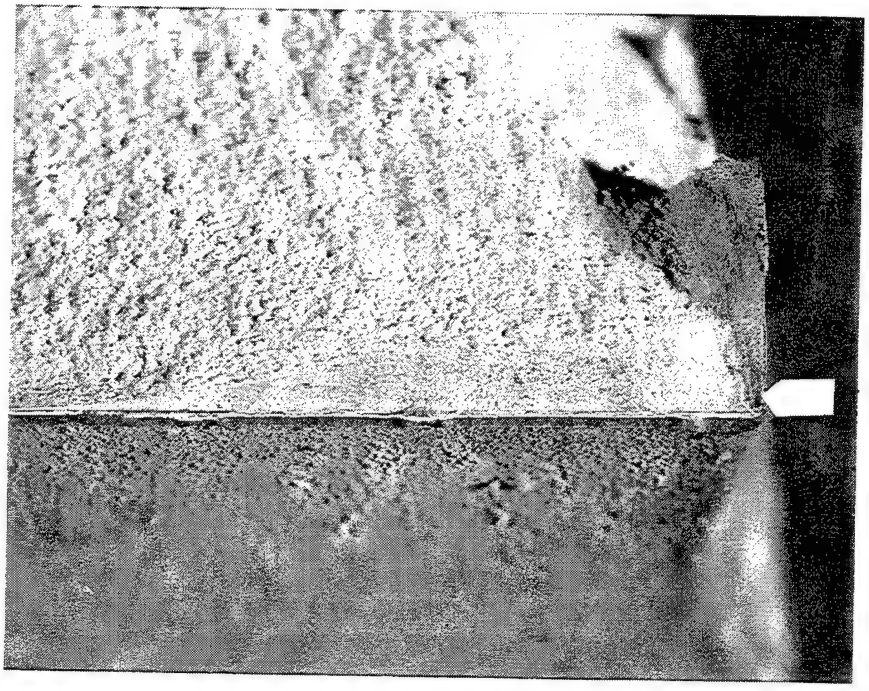

Figure 58. Closeup view of a small fatigue crack (arrow) at B in Figure 53 where it was initiated at the sharp machined fillet (straight edge).

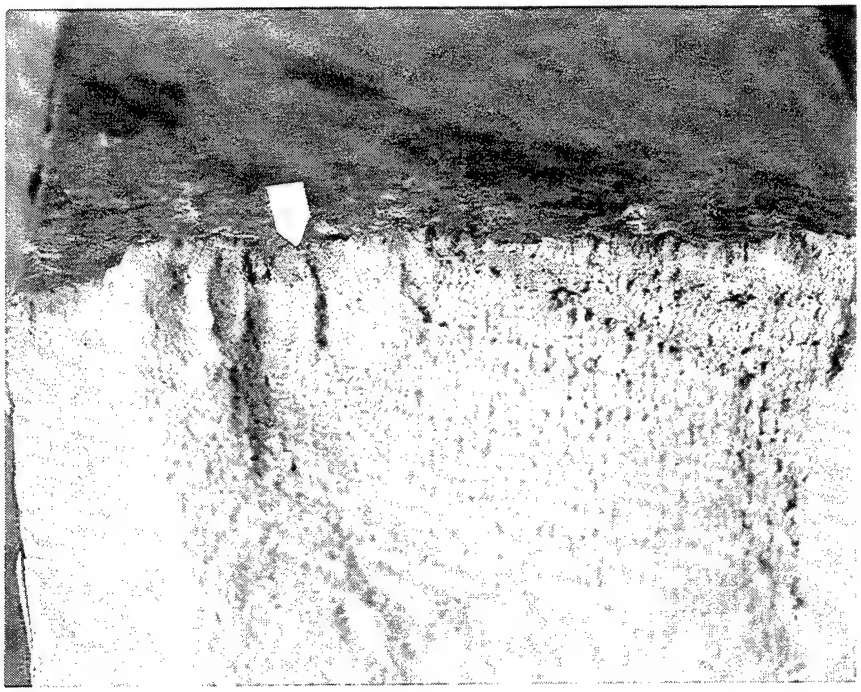

Figure 59. Closeup view of the fracture at A in Figure 54 showing small fatigue cracks (top edge) in the eyehole where the brittle fracture initiated in the connector.

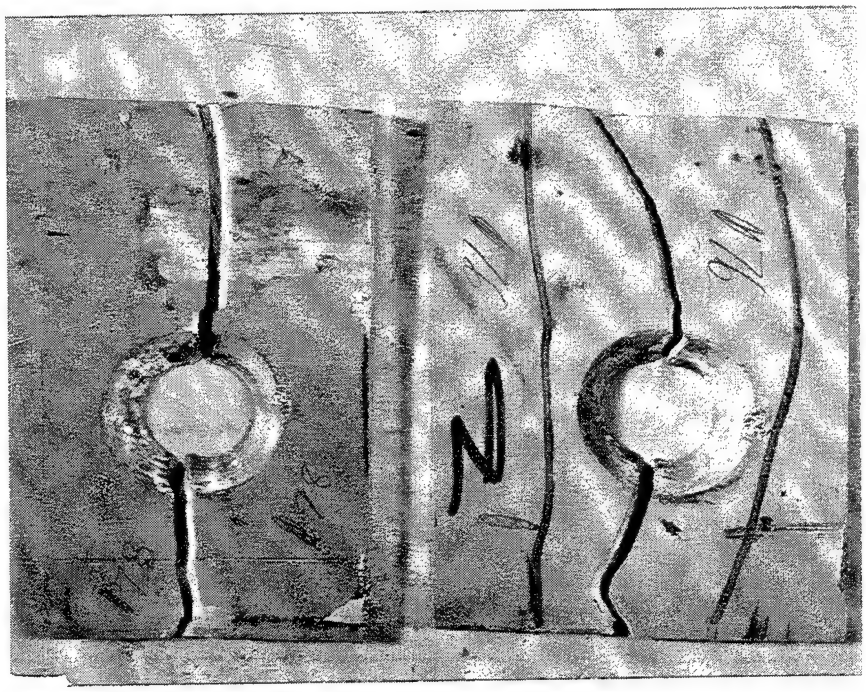

Figure 60. Prior cracks at first countersunk hole of the inner outboard bottom chord angles of the male center panel assemblies that had occurred during the fatigue test of 3,000 simulated MLC-70 tons crossings. See Figure 62 on the extent of corrosion on the surfaces of the other side.

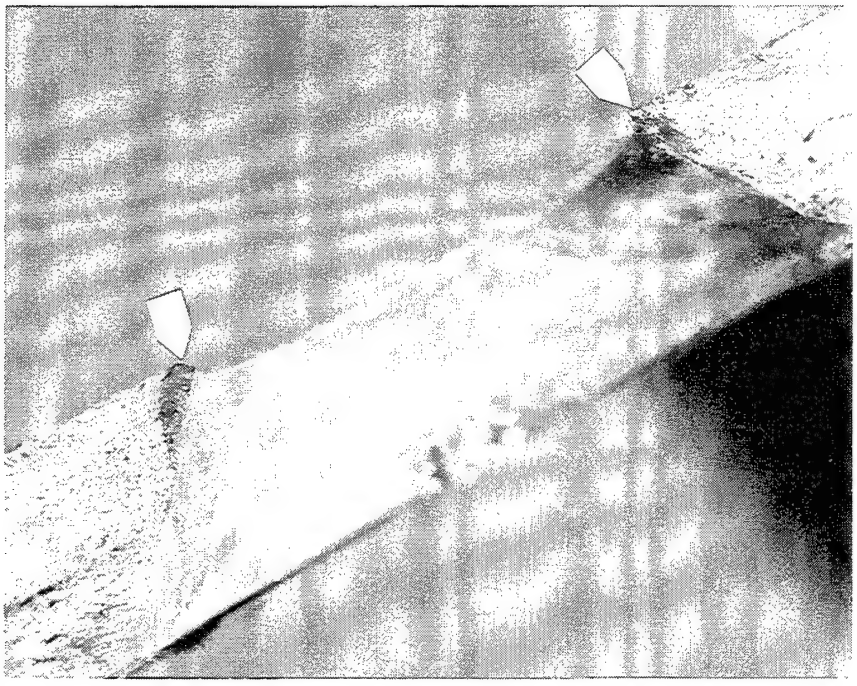

Figure 61. Closeup view of the fracture at the rivet hole of S/N 176 cracked angle leg in Figure 60, showing small cracks at upper corners of the hole. Corrosion may be the initiation sites for the cracks.

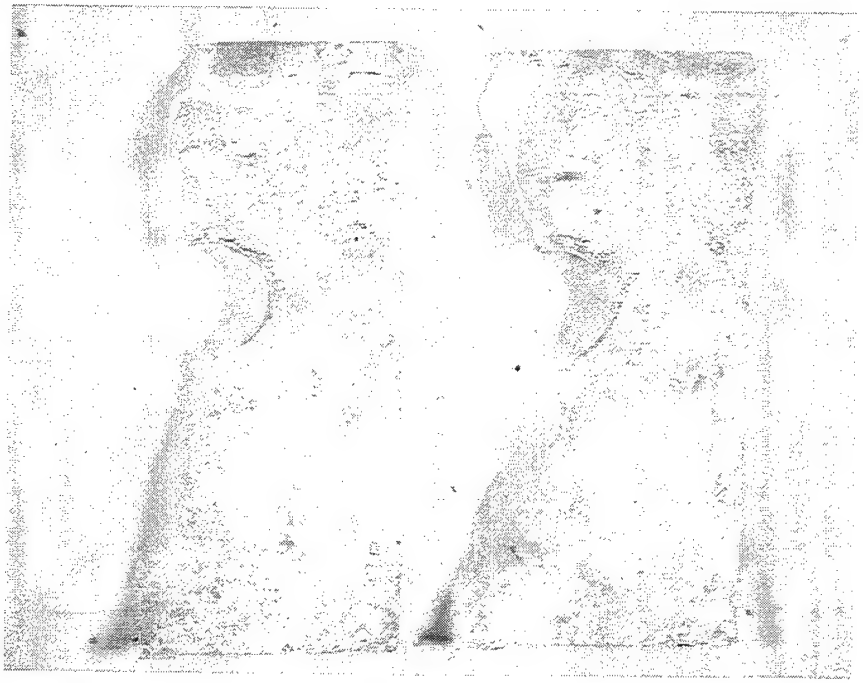

Figure 62. View of the corroded surfaces of the inner outboard bottom chord angles samples cut from the male center panel assemblies S/N 176 and S/N 178 (left) samples in Figure 60. Thick layer of white corrosion products (white areas) is formed on the surfaces that were in contact with the forged center hinges when they were riveted together. Moisture had entered into the gap between two aluminum parts, causing the corrosion.

Small metallographic specimens for microstructural examination were cut from the fractured surfaces of the selected major bridge components in the areas where the cracks initiated. Figure 63 reveals the extensive network of intergranular corrosion at the initiation site of the fatigue crack at point A in Figure 52, the broken inboard female center hinge eye. Figures 64 and 65 show some intergranular corrosion on the corroded surfaces of both bottom chord angle samples in Figure 60 near the crack initiation sites of the fractures in the rivet holes.

Corrosion played an important part in the initiation of small fatigue cracks, which in turn led, with one exception, to brittle fractures of several major aluminum components during the static overload test. Sharp fillets from machining of the outboard bottom male connector created high stress concentration (stress raisers), leading to the initiation of small fatigue cracks that in turn resulted in the brittle fracture of the connector. The fatigue cracks grew to the critical size for the brittle fractures of the aluminum components, made of aluminum alloy 2014, to occur at high loads. Which component failed first, leading to rapid failure of other components, was not determined at that time. It is not clear why catastrophic failure of the bridge did not occur in the bottom chords containing the major cracks that had occurred during the simulated crossings prior to the overload test. Moisture, which may or may not contain chloride ions such as from seawater, had entered in the gaps between components of the bridge to cause corrosion, forming thick white corrosion products on the surfaces in contact with each other.

3. CONCLUSIONS

Based on the results of failure analyses and limited mechanical tests performed on the failed corroded hot-driven aluminum alloy 7277 rivets on the AVLBs from SWA, it is concluded that:

(1) The primary cause of the manufactured head failures of the corroded buttonhead aluminum rivets was due to stress corrosion cracking (SCC) that initiated at the sharp head-to-shank fillets.

(2) Aluminum alloy 7277 used for rivets in hot-driven condition was susceptible to SCC under certain corrosive environmental conditions encountered by the AVLBs, particularly those from SWA.

(3) The cracks in the failed rivet heads followed the grain flow that was formed during the head-forming operation by the rivet manufacturer.

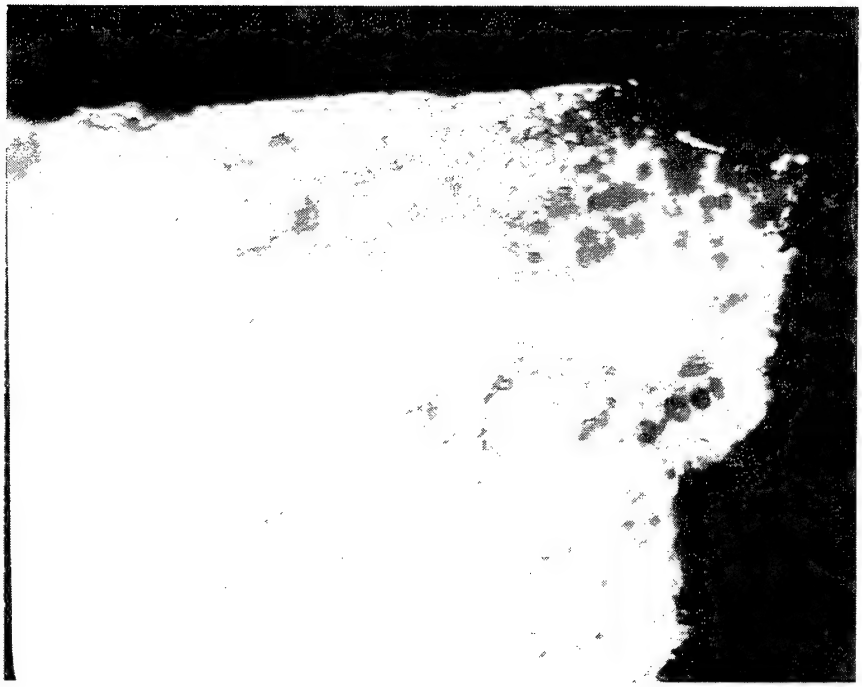

Figure 63. Microstructure of the fracture at A of the broken inboard female center hinge eye in Figure 1.

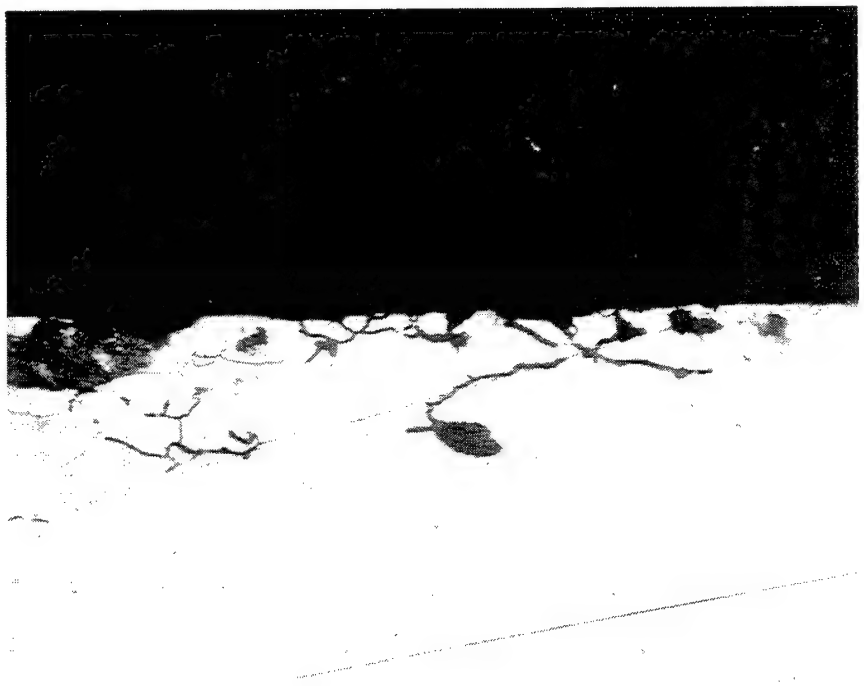

Figure 64. Microstructure of the corroded surface (top edge) near the fracture of the cracked bottom chord angle from male center panel assembly S/N 176 in Figure 62. Note the intergranular corrosion on the surface. Magnification: 160×. As-polished.

Figure 65. Microstructure of the corroded surface (top edge) near the fracture of the cracked bottom chord angle from male center panel assembly S/N 178. Note some intergranular corrosion on the surface. Magnification: 140×. As-polished.

(4) No similar failure of the rivet heads by SCC were found in the driven ends and in the shanks of the failed and corroded buttonhead rivets examined.

(5) Extensive corrosion had occurred in a number of areas on the AVLBs, occurring in the crevices (gaps) between the rivets and rivet holes as well as between other riveted aluminum parts in contact with each other.

(6) Washing down the aluminum AVLBs from SWA by high-pressure spraying with seawater introduced moisture ladened with chloride ions into the crevices of the aluminum parts, possibly accelerating and propagating SCC in the aluminum rivets that led to head failures.

(7) Thick deposits of the white corrosion products were formed, on most occasions, on the failed corroded rivets, particularly in the cracks and on the shanks of the rivets without the head or with cracked head.

(8) Residual stresses were present on hot-driven aluminum rivets on the AVLB, based on the clamping load determinations, possibly playing a role in the initiation of SCC in the sharp fillets, which acted as stress raisers.

(9) Depending on the amounts of the corrosion products on the rivet shanks and rivet holes, the headless corroded rivets can be bound in the holes because of the buildup of the products to the point that they cannot easily be driven out and still function properly when stressed in shear, not in tension, until the bridge can be repaired when possible.

5. RECOMMENDATIONS

ANAD still has a supply of new aluminum alloy 7277 rivets in stock. Those rivets will be used on the Class 60 AVLBs to be overhauled where necessary until the supply of new rivets runs out. A chemical conversion coating from an aerosol spray can will be sprayed into the rivet holes before the hot rivets will be inserted in the holes and hot-driven. Whenever the old, but still usable, riveted AVLB aluminum components have been taken apart or new aluminum components are used to replace the damaged components, a suitable sealant should be applied on the fraying surfaces of the components that will be riveted together to eliminate or minimize corrosion. It was realized that the heat of the hot aluminum rivets would destroy the conversion coating or sealant that may be present in or near the rivet holes.

When the supply of new rivets is gone, ANAD will use another type of fasteners that does away with hot driving as was done on aluminum alloy 7277 rivets. The new fastener is called a Huckbolt fastener (see Figure 66), consisting of an aluminum pin with the locking groves and installation stem and an aluminum collar. "Huckbolt" is a registered trademark of the Huck International, Inc. With the use of the installation tool, the collar is swaged onto the locking grooves of the pin, and the stem is broken off like a familiar "pop" rivet (see Figures 67 and 68).

The commercial Huckbolt fastener that was proposed to replace the hot-driven aluminum rivets had been evaluated in another project for Class 70 AVLB, which is an upgraded version of Class 60 AVLB through a series of modifications. The results of the evaluation will be reported in another ARL technical report in the near future. Meanwhile, a prototype modified Class 70 AVLB has been built at ANAD, having the Huckbolt fasteners in the critical areas. It is now being tested at Aberdeen Proving Ground,

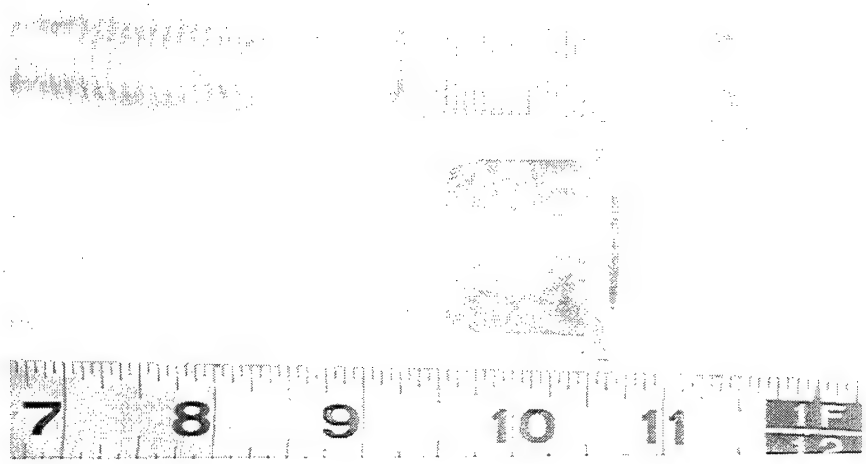

Figure 66. A view of the aluminum Huckbolt fastener. It shows a 0.75-in-diameter pin with the locking grooves next to the pin shank, a grip installation stem at the end of the pin, and a flanged collar.

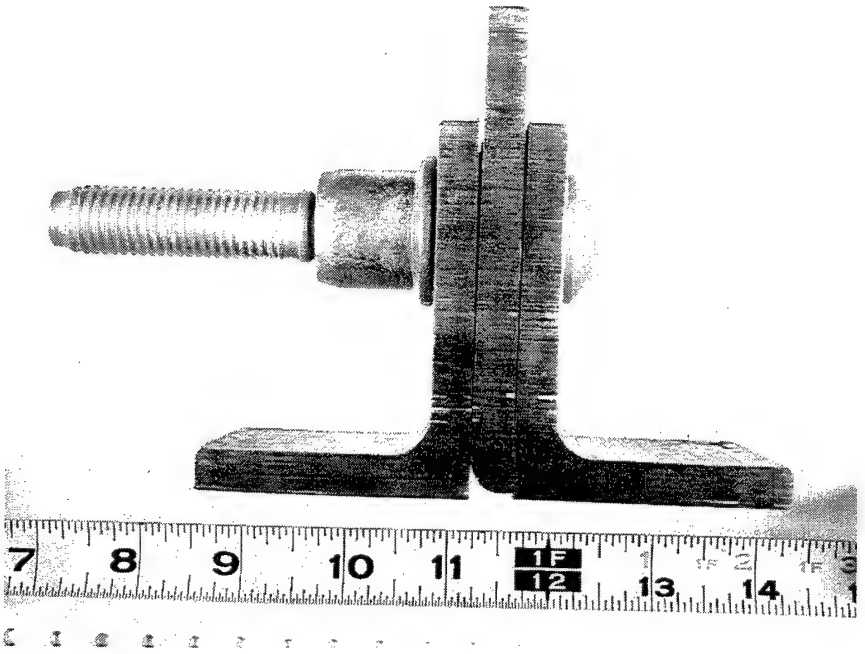

Figure 67. A view of the Huckbolt fastener in the rivet holes of the aluminum parts prior to swaging of the collar. The grip installation stem will be grabbed by the installation tool and broken off after the collar is swaged by the anvil of the tool.

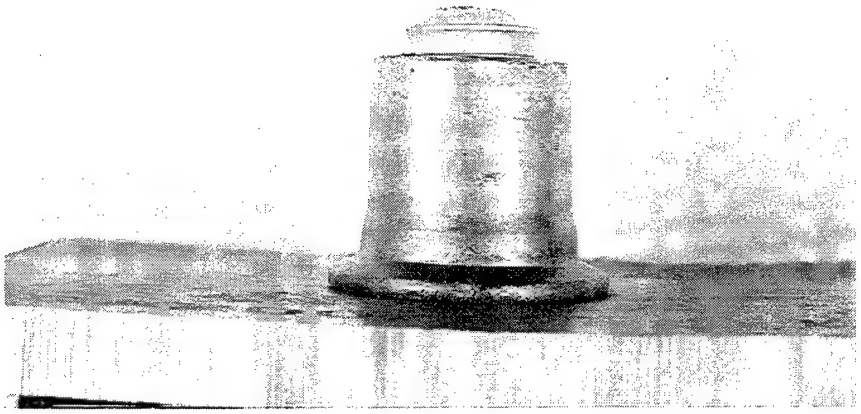

Figure 68. Closeup view of the fully swaged collar of the Huckbolt fastener after the installation. The grip stem of the pin was already broken off.

MD, undergoing Class 70 crossing loads to evaluate new stronger aluminum components and Huckbolt fasteners. Again, chemical conversion coating should be sprayed in the bolt holes for the aluminum Huckbolt fasteners, and a suitable sealant should be applied on the fraying surfaces of the aluminum components to be fastened together.

INTENTIONALLY LEFT BLANK.

NO. OF COPIES	ORGANIZATION
2	DEFENSE TECHNICAL INFO CTR ATTN DTIC DDA 8725 JOHN J KINGMAN RD STE 0944 FT BELVOIR VA 22060-6218
1	HQDA DAMO FDQ ATTN DENNIS SCHMIDT 400 ARMY PENTAGON WASHINGTON DC 20310-0460
1	DIRECTOR US ARMY RESEARCH LAB ATTN AMSRL CS AL TP 2800 POWDER MILL RD ADELPHI MD 20783-1145
1	DIRECTOR US ARMY RESEARCH LAB ATTN AMSRL CS AL TA 2800 POWDER MILL RD ADELPHI MD 20783-1145
3	DIRECTOR US ARMY RESEARCH LAB ATTN AMSRL CI LL 2800 POWDER MILL RD ADELPHI MD 20783-1145
	ABERDEEN PROVING GROUND
2	DIR USARL ATTN AMSRL CI LP (305)

NO. OF
COPIES ORGANIZATION

5 COMMANDER
USA TACOM
ATTN AMSTA TR
WARREN MI 48397-5000

2 DIRECTOR
US ARMY RESEARCH LAB
ATTN AMSRL WM MA
10115 DUPORTAIL RD STE 116
FT BELVOIR VA 22060-5812

ABERDEEN PROVING GROUND

8 DIR, USARL
ATTN: AMSRL-WM (2 CPS)
AMSRL-WM-MA (6 CPS)

USER EVALUATION SHEET/CHANGE OF ADDRESS

This Laboratory undertakes a continuing effort to improve the quality of the reports it publishes. Your comments/answers to the items/questions below will aid us in our efforts.

1. ARL Report Number/Author ARL-TR-1195 (Horner) Date of Report September 1996

2. Date Report Received _____

3. Does this report satisfy a need? (Comment on purpose, related project, or other area of interest for which the report will be used.) _____

4. Specifically, how is the report being used? (Information source, design data, procedure, source of ideas, etc.) _____

5. Has the information in this report led to any quantitative savings as far as man-hours or dollars saved, operating costs avoided, or efficiencies achieved, etc? If so, please elaborate. _____

6. General Comments. What do you think should be changed to improve future reports? (Indicate changes to organization, technical content, format, etc.) _____

CURRENT ADDRESS

_____
Organization

_____
Name

_____
Street or P.O. Box No.

_____
City, State, Zip Code

7. If indicating a Change of Address or Address Correction, please provide the Current or Correct address above and the Old or Incorrect address below.

OLD ADDRESS

_____
Organization

_____
Name

_____
Street or P.O. Box No.

_____
City, State, Zip Code

(Remove this sheet, fold as indicated, tape closed, and mail.)

(DO NOT STAPLE)

DEPARTMENT OF THE ARMY

OFFICIAL BUSINESS

NO POSTAGE
NECESSARY
IF MAILED
IN THE
UNITED STATES

BUSINESS REPLY MAIL
FIRST CLASS PERMIT NO 0001,APG,MD

POSTAGE WILL BE PAID BY ADDRESSEE

DIRECTOR
U.S. ARMY RESEARCH LABORATORY
ATTN: AMSRL-MA-PE
FT BELVOIR VA 22060-5606